Redox Materials for Electrochemical Capacitors

Masanobu Chiku, Mozaffar Abdollahifar, Thierry Brousse, George Z Chen, Olivier Crosnier, Bruce Dunn, Krzysztof Fic, Chi-Chang Hu, Pawel Jeżowski, Adam Maćkowiak, et al.

Electrochemistry
The Electrochemical Society of Japan
Received: May 21, 2024
Accepted: July 2, 2024
Published online: July 5, 2024
Issued: July 31, 2024
https://doi.org/10.5796/electrochemistry.24-70054
Review (Invited Paper) *Electrochemistry*, **92(7)**, 074002 (2024)

The 70th special feature "Research Frontiers of Electrochemical Capacitors"

Redox Materials for Electrochemical Capacitors

OPEN ACCESS

Masanobu CHIKU,[a,*,§] Mozaffar ABDOLLAHIFAR,[b] Thierry BROUSSE,[c,d] George Z. CHEN,[e] Olivier CROSNIER,[c,d] Bruce DUNN,[f] Krzysztof FIC,[g] Chi-Chang HU,[h] Paweł JEŻOWSKI,[g] Adam MAĆKOWIAK,[g] Katsuhiko NAOI,[i,§§] Nobuhiro OGIHARA,[j,§] Naohisa OKITA,[i,§] Masashi OKUBO,[k,§] Wataru SUGIMOTO,[l,m,§§] and Nae-Lih WU[n]

[a] *Department of Applied Chemistry, Osaka Metropolitan University, 1-1 Gakuen-cho, Naka-ku, Sakai, Osaka 599-8531, Japan*
[b] *Department of Materials Science, Faculty of Engineering, Kiel University, Kaiserstraße 2 D-24143, Kiel, Germany*
[c] *Institut des Matériaux de Nantes Jean Rouxel, IMN, Nantes Université, CNRS, 2 rue de la Houssinière BP32229, Nantes cedex 3, 44322, France*
[d] *Réseau sur le Stockage Electrochimique de l'Energie (RS2E), CNRS FR 3459, 33 rue Saint Leu, Amiens Cedex 80039, France*
[e] *Department of Chemical and Environmental Engineering, University of Nottingham, Nottingham NG7 2RD, UK*
[f] *Department of Materials Science and Engineering, University of California, Los Angeles, 3121B Engineering V, Los Angeles, CA 90095-1595, USA*
[g] *Institute of Chemistry and Technical Electrochemistry, Poznan University of Technology, Berdychowo 4, Poznan 60-965, Poland*
[h] *Department of Chemical Engineering, National Tsing Hua University, 101, Section 2, Kuang-Fu Road, Hsin-Chu 300044, Taiwan*
[i] *Department of Applied Chemistry, Tokyo University of Agriculture & Technology, 2-24-16 Naka-cho, Koganei, Tokyo 184-8588, Japan*
[j] *Nobuhiro Ogihara Research Group, Frontier Research Management Office, Toyota Central R&D Labs., Inc., 41-1 Yokomichi, Nagakute, Aichi 480-1192, Japan*
[k] *Department of Electrical Engineering and Bioscience, Waseda University, 3-4-1 Okubo, Shinjyuku-ku, Tokyo 169-8555, Japan*
[l] *Research Initiative for Supra-Materials (RISM), Shinshu University, 3-15-1 Tokida, Ueda, Nagano 386-8567, Japan*
[m] *Faculty of Textile Science and Technology, Shinshu University, 3-15-1 Tokida, Ueda, Nagano 386-8567, Japan*
[n] *Department of Chemical Engineering, National Taiwan University, No. 1, Section 4, Roosevelt Rd, Da'an District, Taipei 10617, Taiwan*

* *Corresponding author: chiku@omu.ac.jp*

ABSTRACT

Electrochemical capacitors are known for their high power density and cyclability, and various redox reactions can be utilized to improve their energy density. A great variety of redox materials have been investigated recently for use in electrochemical capacitors, not only transition metal oxides, which have been studied for many years. In this review, we provide a comprehensive explanation of redox materials for electrochemical capacitors. Manganese oxides and ruthenium oxides, which are typical metal oxides exhibiting pseudocapacitance, are first discussed. Nickel oxides used in hybrid capacitors are also covered. Various 0D and 2D nanomaterials are highlighted. Pseudo-capacitance using nanosized complex materials and metal-organic frameworks is also presented. Furthermore, electrolyte systems that exhibit redox characteristics for electrochemical capacitors are also reviewed.

Keywords : Electrochemical Capacitor, Pseudo Capacitor, Redox Material

§ECSJ Active Member
§§ECSJ Fellow
M. Chiku orcid.org/0000-0002-2156-1785
M. Abdollahifar orcid.org/0000-0002-4440-4141
T. Brousse orcid.org/0000-0002-1715-0377
G. Z. Chen orcid.org/0000-0002-5589-5767
O. Crosnier orcid.org/0000-0001-6747-9413
B. Dunn orcid.org/0000-0001-5669-4740
K. Fic orcid.org/0000-0002-5870-7119
C.-C. Hu orcid.org/0000-0002-4308-8474
P. Jeżowski orcid.org/0000-0001-9869-0641
A. Maćkowiak orcid.org/0000-0001-9380-2974
K. Naoi orcid.org/0000-0002-0265-2235
N. Ogihara orcid.org/0000-0002-6305-6859
N. Okita orcid.org/0000-0003-4683-3991
M. Okubo orcid.org/0000-0002-7741-5234
W. Sugimoto orcid.org/0000-0003-3868-042X
N.-L. Wu orcid.org/0000-0001-6545-8790

Masanobu Chiku (Associate Professor, Graduate School of Engineering, Osaka Metropolitan University)

Masanobu Chiku was born in 1981. He received his Ph. D. in Engineering from Keio University in March 2010. He joined Osaka Prefecture University in 2010 and was promoted to Associate Professor in 2018. He was awarded the Awards for The Committee of Battery Technology from the committee of battery technology in the electrochemical society of Japan in 2018.
His research interests are battery, capacitor, and electrochemical analysis. Hobby: Theater-going.

1. Introduction

Research involving the development of redox materials for electrochemical capacitors has witnessed exceptional growth over the past decade. The roots of this research area are the prototypical materials RuO_2 and MnO_2, both of which are based on the change in oxidation state in aqueous electrolytes. With the extraordinary development of lithium-ion battery technology over the past two decades, this has led to the development of redox materials along with widespread availability of non-aqueous lithium electrolytes. It was, perhaps, inevitable that there would be crossover as researchers would begin to create and rediscover materials whose properties intertwined battery and electrochemical characteristics. The benefit of this new direction is the prospect of creating new generations of materials which exhibit redox-based charge storage processes that operate at the charge and discharge rates typically shown by electrical double layer capacitors (EDLCs).

As demonstrated in this review, the range of materials has expanded well beyond the initial group of oxides. RuO_2 and MnO_2 represent the core of the field and continue to be actively studied as they play an important role in providing benchmarks of material performance as well as being incorporated in energy storage devices. However, there are a wide range of inorganics including oxides, carbides, nitrides and sulfides in which redox reactions occur at high rates, well above those of typical battery materials. An important consideration with these materials systems is the layered structures that occur in transition metal oxides, dichalcogenides and MXenes. The two-dimensional (2D) crystallographic pathways in these structures provide a wealth of available sites for mobile ion intercalation while the blocks adjacent to the layers contain the transition metals that carry out redox reactions which lead to charge storage. Organic materials represent another important category of redox materials for electrochemical capacitors. In the 1980's conducting polymer films were widely investigated as they exhibited finite diffusion properties and played important roles in demonstrating how increasing electrode potential led to continuous changes in oxidation state. The more recent development in this area is that of developing metal-organic framework (MOF) materials. These materials have extraordinary design capabilities as organic and inorganic functionalities are integrated and able to form self-assembled structures with pore networks. Although the MOF-based research direction has only emerged in the past few years, there have been some significant advances, leading to the development of systems whose theoretical capacity is comparable to battery electrodes.

Nanoscale materials constitute another vital contribution to the field. From a kinetic standpoint, these materials benefit from thin

Mozaffar Abdollahifar (Group leader, Faculty of Engineering, Kiel University, Germany)

He received his PhD from National Taiwan University (NTU) in 2018, where he focused on developing supercapacitors and lithium-ion battery materials. Since then, he has held various research positions in Taiwan and Germany for several years, before being appointed as a group leader for batteries/supercapacitors. He is the recipient of numerous (inter)national awards.
His research interests are battery and supercapacitor materials and electrodes.
Hobby: Mountain climbing.

Thierry Brousse (Professor, Polytech Nantes, Institut des Matériaux de Nantes Jean Rouxel-IMN, CNRS/Nantes Université)

Dr. Thierry Brousse was born in 1965. He received his PhD in 1991 from ISMRa Caen. His research topics are materials for supercapacitors, high power batteries and related microdevices. He organized the first ISEECap meeting in 2009 (International Symposium on Enhanced Electrochemical Capacitors) which is now taking place every two years. He has been appointed Fellow of the International Society of Electrochemistry in 2022.
Prof. Brousse was also the Vice-Dean of Nantes Université in charge of Innovation from 2013 to 2020, and in 2024 he took the position of Director in charge of Research and International Partnerships at Polytech Nantes.

George Zheng Chen (Professor of Electrochemical Technologies, Dept. of Chemical and Environmental Eng, University of Nottingham, UK)

George obtained his MSc and PhD degrees in Fujian Normal University (1985) and Imperial College London (1992), respectively. Since 1985, he worked in various universities in China (Nanchang, Wuhan and Ningbo) and the UK (Oxford, Leeds, Cambridge and Nottingham). He has authored over 310 peer reviewed articles in journals and books and 200 invited lectures at conferences and seminars under the research theme of electrochemical technologies and liquid salts innovations for materials, energy and environment with a focus on supercapattery, supercapacitor and battery.

Olivier Crosnier (Assistant Professor, CNRS-IMN, Nantes University)

Olivier Crosnier was born in 1974. He is a researcher at the Institut des Matériaux de Nantes Jean Rouxel (IMN) since 2007. His research focuses on materials for electrochemical energy storage with particular emphasis on innovative and/or modified materials for electrochemical capacitors and high power batteries.

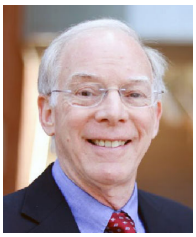

Bruce Dunn (Nippon Sheet Glass Professor, Materials Science and Engineering, UCLA)

His research interests concern the synthesis of inorganic and organic/inorganic materials, and the characterization of their electrical, optical, biological and electrochemical properties. His recent work on electrochemical energy storage includes three-dimensional batteries and pseudocapacitive materials. Among the honors he has received are a Fulbright research fellowship, the Orton Lectureship from the American Ceramic Society, named to the Web of Science list of Highly Cited Researchers, and awards from the Department of Energy for outstanding research in materials science.

Krzysztof Fic (Associate Professor, Poznan University of Technology, Poland; Lukasiewicz Research Network – IMN Gliwice/Poznan, Poland and Visiting researcher at Kansai University, Japan)

Krzysztof Fic was born in 1984. He graduated in chemical engineering from Poznan University of Technology in June 2008 and earned Doctor of Science in June 2012 (electrochemistry). In 2020 he was promoted to Associate Professor.
He was awarded Young Investigator Award from The Energy Storage Materials journal in 2018. His research interests are materials for fast electrochemical energy storage, especially electrolytes with redox activity.
Hobby: philosophy, prime numbers, Japanese culture understanding and exploration.

layer electrochemistry where $l \ll (Dt)^{1/2}$ where the ion diffusion length is l, the diffusion coefficient is D and t is diffusion time. In thin-layer electrochemistry, the faradaic reactions occur within a finite diffusion space where concentration gradients which occur in the bulk electrode are negligible and redox kinetics begin to resemble capacitive processes. The use of thin films, nanoparticles and even exfoliated layers benefit from redox reactions occurring at or near the surface. The resulting materials possess fast kinetics in that charge and discharge reactions occur at a time scale normally observed with EDLCs, only now the charge storage is at least an order of magnitude greater.

Although the redox materials being developed for electrochemical capacitors differ in terms of their chemistry and structure, there are a number of commonly observed features that we often term 'signatures'. As with any pseudocapacitive material, we expect that an incremental change in stored charge, Q, will occur with a change in voltage, V, i.e., dQ/dV, gives a nearly linear response. This gives rise to a defining feature of a pseudocapacitive material, that a linear dQ/dV is accompanied by faradaic charge storage that is not limited by diffusion. Thus, the energy stored $E = 1/2\ CV^2 = 1/2\ QV$. That is, the stored energy is changing continuously as charge is added incrementally. In contrast, a battery material is characterized by having the majority of the charge being stored at a constant potential. An important consideration for electrochemical capacitors is that the linear dQ/dV is not susceptible to the concentration polarization behavior which frequently limits battery materials at the end of discharge.

The contributions to this review provide a good representation of the status of the redox materials being investigated for electrochemical capacitors. The contributions by Abdollahifar and Wu on the MnO_2 polytypes and Sugimoto on RuO_2 provide a good sense of the state of our understanding of structure-property relationships for these classic materials. The contribution by Brousse and Crosnier gives an excellent perspective of other oxides which exhibit capacitive-like electrochemical signatures and how this relates to the seminal work by Trasatti and Conway. Among the non-oxide systems, the overview by Okubo on MXenes presents both the advantages and the limitations of this family of materials. Ogihara's review of the recent progress in the energy storage properties of MOFs underscores the exceptional design capabilities for these organic-inorganic systems while the discussion by Hu shows the advantages of using a variety of different nanoscale materials for energy storage. Finally, the contribution by Fic and co-workers makes an important point that is easily overlooked. That is, redox

Chi-Chang Hu (Chair Professor, Department of Chemical Engineering, National Tsing Hua University)

Chi-Chang Hu was born in 1969. He grauated from Department of Chemical Engineering, National Cheng Kung University in July 1995, and earned PhD in Engineering, He worked in National Chung Cheng University in 1997–2007 for being assistant, associate, and full professors. He moved to National Tsing Hua University as a full professor in 2007 and became distinguished professor in 2011 and chair professor in 2014. He was awarded Thomson Scientific Citation Laureate in 2006 and Tajima Prize from The International Society of Electrochemistry in 2007. Now, he serves as the President of the Electrochemical Society of Taiwan. His research interests include electrochemical energy storage devices, electrochemical separation, and electroplating. Hobby: swimming, table tennis, and sing songs.

Paweł Jeżowski (Assistant Professor, Graduate School of Engineering, Poznan University of Technology)

Paweł Jeżowski was born in 1988. He graduated from Engineering, Poznan University of Technology in November 2016, and earned a Doctor of Science, He joined Poznan University of Technology in 2016 and was promoted to assistant professor in 2017. He was awarded the best presentation award from The Electrochemical Society in 2015. His research interests are material science, electrochemistry & food chemistry. Hobby: video games & active sports.

Adam Maćkowiak (Assistant, Graduate School of Engineering, Poznan University of Technology)

Adam Maćkowiak was born in 1995 in Poland. He received his Master and Engineering degrees from the Poznan University of Technology. He is a PhD student and assistant researcher involved in the European Research Council Starting Grant and Proof of Concept grant supervised by Dr. Krzysztof Fic. His works focuses on developing a one-step assembly method for metal-ion capacitors.
His research interests include Li-ion and Na-ion batteries and capacitors. Hobby: traveling, sailing, racketlon.

Katsuhiko Naoi (Emeritus Professor, Tokyo University of Agriculture and Technology)

Katsuhiko Naoi, an Emeritus Professor at Tokyo University of Agriculture and Technology (TUAT), stands as a distinguished authority in the realm of "Supercapacitor". Boasting a PhD from WASEDA University, a post-doctoral stint at the University of Minnesota, and valuable industry experience at BASF in Germany, his illustrious career has solidified his position as a global leader in the field. Notably, in 2012, he established the world's pioneering strategic center for "Supercapacitor," showcasing his commitment to advancing the frontiers of knowledge. His visionary leadership has fostered innovation and collaboration within the supercapacitor domain and beyond.

Nobuhiro Ogihara (Principal Researcher, Nobuhiro Ogihara Research Group, Toyota Central R&D Labs., Inc.)

Nobuhiro Ogihara was born in 1976. He received his Ph. D. in Engineering from Tokyo University of Agriculture and Technology (TUAT) in 2005. He worked in TUAT in 2005–2008, as Assistant Professor. He moved to Toyota Central R&D Labs., Inc., in 2008 and promoted to Principal Researcher in 2020. He was awarded the Awards for The Committee of Battery Technology from the committee of battery technology in the electrochemical society of Japan in 2016.
His research interests are electrochemical applications. Hobby: Speed Cube.

Naohisa Okita (Assistant Professor, Tokyo University of Agriculture and Technology)

Naohisa Okita was born in 1991. He received his Ph.D. in Engineering from Tokyo University of Agriculture and Technology in March 2019. He worked as assistant professor for Tokyo University of Agriculture and Technology from 2019. He founded RING-e Co., Ltd., a university start-up company in 2023. His research interests are next generation supercapacitors and superbatteries, as well as fusion of plant, microbe and electrochemistry. Hobby: Running and rice-farming.

properties are not limited to solid-state materials and that redox-active electrolytes represent a viable alternative. Taken together, these contributions show the rich chemistry that serves as the basis for creating redox materials for electrochemical capacitors. In moving beyond the initial MnO_2 and RuO_2 systems to new generations of materials, the field has emerged as one of the most promising approaches for achieving energy storage materials possessing high energy density at high rates. There is little doubt that the importance of such energy storage materials is certain to grow in the immediate future.

2. Classification of Surface Redox Active Compounds

2.1 Overview of oxides that exhibit fast/surface redox process

The early research work of Trasatti et al. in 1971[1] on the use of RuO_2 as a potential material to challenge activated carbon electrodes in electrochemical capacitors led to the main question of how a "capacitive-like" behavior can find its origins in redox surface reactions. B. E. Conway proposed that in such oxides *"capacitance arises on account of the special relation that can originate for thermodynamic reasons between the extent of charge acceptance (ΔQ) and the change of potential (ΔV), so that a derivative* d*(ΔQ)*/d*(ΔV), which is equivalent to a capacitance, can be formulated and experimentally measured by dc, ac, or transient techniques"*. This triggered the wording « pseudocapacitive charge storage » which was then used to designate electrodes exhibiting a capacitive-like signature but with calculated capacitances which exceeded by one or two order of magnitudes those observed for double layer capacitance of moderate surface area oxides (10–200 $m^2\,g^{-1}$).[2–4]

The faradaic reactions occurring at the surface of the so-called pseudocapacitive electrodes upon cycling were evidenced by *in-situ*[5–9] and/or *operando* techniques.[10,11] These studies were especially designed to demonstrate clearly the change of oxidation state of the electroactive cation in manganese dioxide based electrodes operated in mild aqueous electrolytes, following the first report from Lee and Goodenough on the pseudocapacitive behavior of MnO_2 in such electrolytes.[12,13]

After these early studies, several compounds such as $FeWO_4$[14] or VN[15] have been investigated in the same way, leading to the same conclusions, i.e. that a capacitive like electrochemical signature can be associated with faradaic reactions taking place over the investigated potential window instead of occurring at a given potential. However, at some stage this peculiar charge storage mechanism was extrapolated to materials that were clearly battery type electrodes, thus leading to a number of controversial papers in the literature.[16,17] Importantly, for several decades, pseudocapacitive behavior was associated with the use of aqueous based electrolytes and the role of protons.[18] The story became more confusing when oxides operated in organic based electrolytes exhibited a capacitive-like behavior, such as Nb_2O_5, leading to new wording such as "intercalation pseudocapacitance" and many others less appropriate.[19,20]

Despite the significant number of electrode materials reported in the literature, few of them demonstrate "pure" pseudocapacitive behavior and most of the materials depicted as pseudocapacitive clearly show a mixture of pseudocapacitance and battery-type behavior. Very recently, Fontaine and co-workers proposed a method to determine the percentage of pseudocapacitance vs battery-type behavior[21] and provided the electrochemical evidence of how pseudocapacitance arises in a given material as well as the factors promoting such behavior.[22] There is no doubt that the tools developed and proposed to researchers within the framework of these two studies will greatly help the scientific community to understand the electrochemical behavior of new electrode materials and to focus on research directions that can promote either energy density or power density, or a tradeoff between the two, while tailoring new electrode materials.

2.2 Manganese oxides

Manganese (Mn), being a transition metal, has the unique property of existing in various forms of stable oxides, including MnO,[23] Mn_3O_4,[24] Mn_2O_3,[25] and MnO_2[12,26] with remarkable pseudocapacitive behavior, which makes them ideal for use in energy storage applications. In particular, MnO_2 has gained significant interest because of its excellent electrochemical performance. As mentioned in section 2.1, in 1999, Lee and Goodenough[12] demonstrated that amorphous MnO_2 electrodes exhibit excellent pseudocapacitive behavior in mild electrolytes, which was followed in 2002 by Hong et al.[27] who developed a 2.0 V aqueous capacitor using MnO_2 and activated carbon as the electrode materials. Subsequent studies by Toupin et al.,[7,13] encouraged the research community to explore high-performance electroactive MnO_2 as a highly attractive electrode material. MnO_2 is a low-cost, abundant resource, which is environmentally benign and possesses a high theoretical specific capacitance of 1370 $F\,g^{-1}$, based on the single-

Masashi Okubo (Professor, Department of Electrical Engineering and Bioscience, School of Advanced Science and Engineering, Waseda University)

Dr. Okubo received a Ph.D. in coordination chemistry from the University of Tokyo in 2005. After serving as a postdoctoral fellow, an assistant professor, a senior researcher, and an associate professor at Université Pierre et Marie Curie, National Institute of Advanced Industrial Science and Technology, and the University of Tokyo for 16 years, he was appointed as a professor at Waseda University, where he is now. His research interest focuses on the development of electrochemical energy storage devices.
Hobby: Travel, Wine, Shogi

Wataru Sugimoto (Distingushied Professor, Faculty of Textile Science and Technology and Research Initiative for Supra-Materials, Shinshu University)

Dr. Wataru Sugimoto received his PhD degree in 1999 from Waseda University and has been a Professor of Materials and Chemical Engineering at Shinshu University since 2013 (appointed Distinguished Professor in 2019). His research focuses on nano-materials for electrochemical charge storage and conversion with particular emphasis on the synthesis of conductive nanosheets targeted towards electrochemical energy storage and conversion. He has received several awards including the The Commendation for Science and Technology by the Minister of Education, Culture, Sports, Science and Technology, Awards for Science and Technology, Research Category in 2023, Oronzio De Nora Foundation Prize of The International Society of Electrochemistry on Electrochemical Energy Conversion in 2005 and the Scientific Achievement Award from The Electrochemical Society of Japan in 2018. He is a Fellow of The Electrochemical Society of Japan.

Nae-Lih Wu (Professor, Chemical Engineering Department, National Taiwan University)

Nae-Lih Wu was born in 1958. He grauated from Chemical Engineering Department, Pennsylvania State University in 1988, and earned PhD. His research interests include (1) electrochemical energy storage devices, including supercapacitors and rechargeable batteries; (2) nano-materials synthesis and applications; and (3) advanced synchrotron X-ray spectroscopy analyses for energy materials.

electron redox reaction between $Mn^{(IV)}$ to $Mn^{(III)}$ that is responsible for its pseudocapacitive behavior. In addition, a wide electrochemical potential window of about 1.0 V (with surface modifications can be extended from −1.0 to 1.0 V)[28] while the ability to use neutral aqueous electrolytes, reduces chemical corrosion of the current collectors compared to strong acid/basic electrolytes. Although MnO_2-based electrodes have the potential to be a safe and cost-effective substitute for current commercial EDLCs, MnO_2 often shows lower specific capacitances for thick electrodes[29,30] made with powders. However, for thin films with very low electrode loading, the capacitance can achieve values close to the theoretical capacitance.[7,13,31,32] Besides electrode design and loadings, the low real capacitance of MnO_2 could be also attributed to its crystalline structure, electrolyte properties, material morphologies, and electrode conductivity (which depends on the amount and type of conductive carbon and binder).

MnO_2 Structures: The diversity of MnO_2 structures and valence is a result of the basic MnO_6 octahedron, which can be linked together to form endless chains of MnO_6 octahedral subunits, and connect to neighboring chains to construct 1D, 2D, or 3D tunnels among other structures (Fig. 1a). These tunnels could be filled with foreign cations or water molecules,[33,34] which force $Mn^{(IV)}$ ions to become $Mn^{(III)}$ ions to balance the charge. Thus, the cationic properties of MnO_2, coupled with the reversible transition between $Mn^{(III)}$ and $Mn^{(IV)}$, makes it an ideal material for electrochemical energy storage (EES).

Charge Storage Mechanism: The reaction mechanism for MnO_2 involves surface and/or bulk redox/Faradaic reactions that occur in two stages: (i) adsorption/desorption of alkali metal cations (A^+), including Li^+, Na^+, and K^+, on the material surface (Reaction 1). This mechanism typically occurs with amorphous and poorly crystalline structures. In stage (ii), there is insertion/extraction (or intercalation/deintercalation) of A^+ and protons (H^+) into/out of the bulk material (Reaction 2, Reaction 3) as usually occurs with crystalline structures. As a result, the pseudocapacitive behavior of MnO_2 polymorphs is greatly impacted by their crystallographic structures, as well as the type of cations involved in the charge storage process (Fig. 1). Toupin et al.[7] demonstrated that the charge storage mechanism for thick MnO_2 composite electrodes is based on electrostatic effects, similar to carbon electrodes, as only a thin layer is involved in the charge storage process in which the Mn oxidation state varied from (III) to (IV) during (dis)charge in thin film electrodes. They also showed that Na^+ cations from electrolytes were involved in charge storage, but the Na/Mn ratio was low for reduced electrodes, suggesting the involvement of protons in the pseudo-faradaic mechanism. More information regarding the charge storage mechanism is shown in Figs. 1g–1i. In aqueous electrolytes, the general (dis)charge mechanism for MnO_2-based electrodes could be explained by the following reactions:[7]

$$(MnO_2)_{surface} + A^+ + e^- \leftrightarrow (MnO_2{}^-A^+)_{surface} \quad (1)$$

$$MnO_2 + A^+ + e^- \leftrightarrow MnOOA \quad (2)$$

$$MnO_2 + H^+ + e^- \leftrightarrow MnOOH \quad (3)$$

Recently, defect engineering has emerged as a useful method to modify the fundamental physicochemical properties of MnO_2 and other oxide materials.[35,36] Among various methods, introducing oxygen vacancies through different techniques has been found to have a significant effect as it enhances electrical conductivity and creates a local electric field, which helps to facilitate the transfer of interfacial electrons/ions.[37–40]

2.3 Ruthenium oxides

2.3.1 Background

Ruthenium oxide (RuO_2) is considered as a 'model' electrode material for the mechanistic understanding behind the pseudocapacitive properties of oxide electrodes. RuO_2 is one of the few oxides with metallic conductivity, electrocatalytic activity, and excellent corrosion resistance in both acidic and basic electrolytes, thus has found use as the main component of chlorine generation anodes for industrial electrolysis. Trasatti and Buzzanca[42] were the first to recognize that the rectangular box-like shaped CV curve of a RuO_2 film resembled that of the carbon-based EDLC. Porous carbons are electrochemically inert due to the absence of redox process and thus behave as an ideally polarizable system, i.e. charge storage originates only from the non-Faradaic electrical double layer charging. On the other hand, the presence of surface or near-surface-confined redox for RuO_2 leads to additional charge storage. If the charge transfer resistance of the surface-confined redox process is small, the kinetics are extremely fast and exhibits reversible or pseudo-reversible behavior leading to the term and concept "pseudo-capacitor".

A quarter of a century after the discovery of pseudocapacitive behavior of RuO_2,[1] Zheng et al. reported record-breaking specific capacitance with hydrous RuO_2 nanoparticles prepared by a sol-gel method.[42,43] This epoch-making study activated a world-wide surge in the study of RuO_2-based electrodes for electrochemical capacitor application and RuO_2 nanomaterials are considered as the '*gold standard*' of pseudocapacitive materials. If RuO_2 is made into nanoparticles of 1 to 2 nm to increase the surface area (theoretical specific surface area of c.a. 200 $m^2\,g^{-1}$), a specific capacitance of 600 to 800 $F\,g^{-1}$, or in some cases over 1,000 $F\,g^{-1}$, can be obtained.[44–46] As a result, much of the research and development effort has emphasized structure-property relations. Higher capacitance and enhanced power capability has been achieved by material design, and sophisticated characterization methods have contributed to the understanding of the Faradaic (and non-Faradaic) charge storage of RuO_2-based electrodes. Owing to such extensive studies, the fundamental charge storage properties of RuO_2 are now much better understood.

2.3.2 Theoretical capacitance of RuO_2

After 50 years of fundamental research, we now have a fairly clear picture on the charge storage mechanism behind the pseudocapacitive charge storage mechanism of RuO_2-based electrodes. As the charge storage is surface confined, the mass specific capacitance depends on the specific surface area and therefore is a function of the particle size.[44] The most widely reported specific capacitance value for RuO_2 is 80 $\mu F\,cm^{-2}$ [47–50] which is considerably larger than the value of ~20 $\mu F\,cm^{-2}$ observed with a mercury electrode in a diluted aqueous electrolyte solution.[51] Using this 80 $\mu F\,cm^{-2}$ value as a probe and assuming spherical particles, the mass specific capacitance can be calculated from the specific surface area. As shown in Fig. 2a, the calculated mass specific capacitance for RuO_2 particles with a diameter of 1 nm is 680 $F\,g^{-1}$.[44] This matches with the experimentally reported mass specific capacitance of sol-gel derived RuO_2 nanoparticles of 1 to 1.5 nm in diameter.[42,43,52,53] It should be noted that the probe value of 80 $\mu F\,cm^{-2}$ should include contribution from both electrical double layer charging (non-Faradaic) and surface confined redox processes (Faradaic). It is quite challenging to experimentally differentiate between the contribution from the electric double-layer capacitance C_{dl} and redox-related Faradaic capacitance C_{redox}, as the (surface) redox related pseudo-capacitance for RuO_2 is a fast and reversible process. Such efforts have been reported using various electrochemical measurements including rotating disk electrodes (RDE),[50,54] electrochemical impedance spectroscopy,[55] and step potential electrochemical spectroscopy (SPECS)[56] methods.

The theoretical mass specific capacity can be calculated from Faraday's equation assuming a bulk reaction, i.e. all Ru ions in the crystal structure participate in the reaction.

$$m = \frac{Q}{F} \times \frac{M}{n} \quad (4)$$

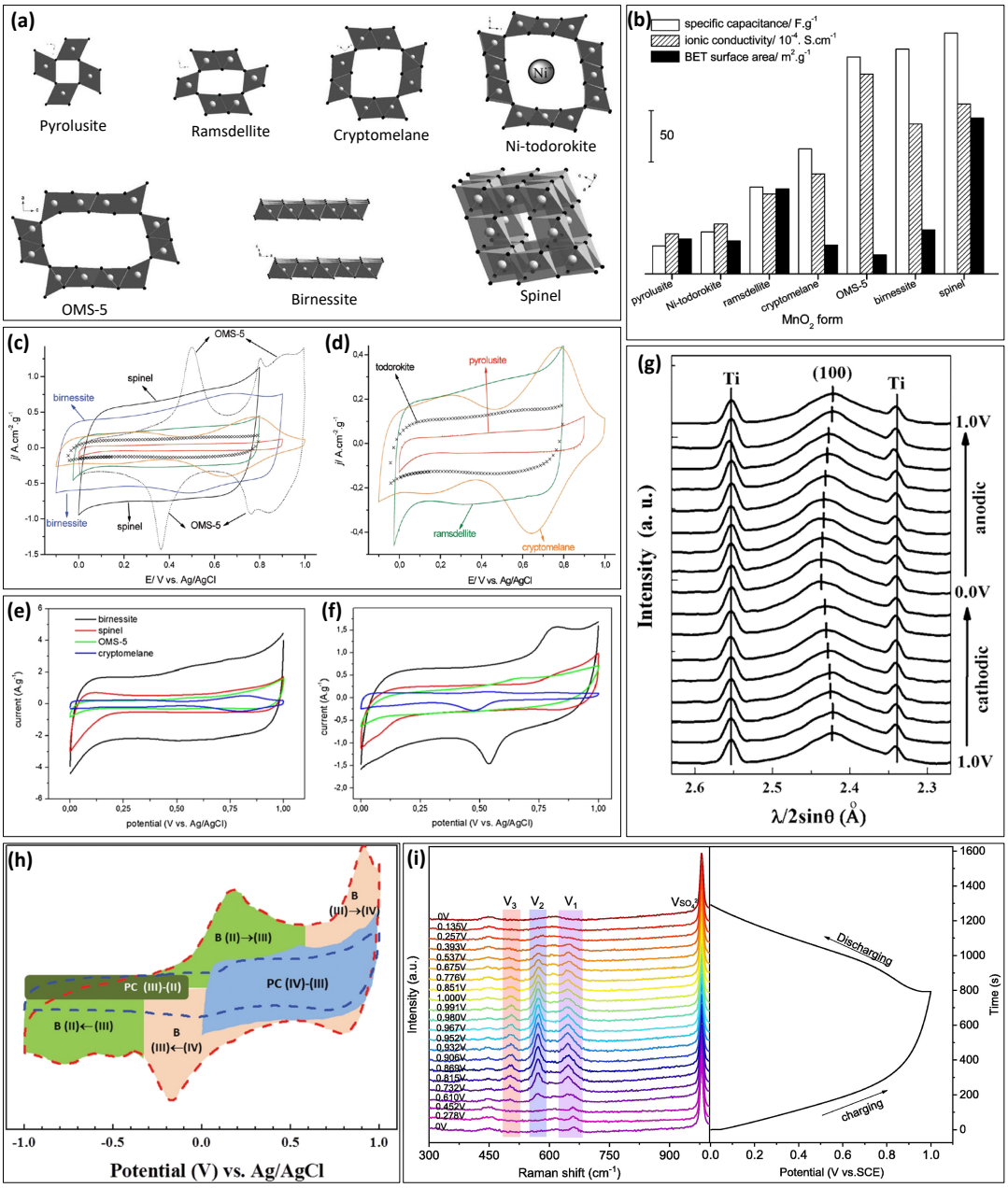

Figure 1. Properties of Mn-based pseudocapacitive electrodes: (a) MnO_2 crystallographic structures, (b) Comparison of MnO_2 structures: capacitance, conductivity, and BET surface area, (c and d) CV curves of various MnO_2 structures at $5\,mV\,s^{-1}$ in aqueous $0.5\,M\ K_2SO_4$,[31] reprinted with permission from Ref. 31. Copyright 2009 American Chemical Society. CV curves of some MnO_2 structures at $5\,mV\,s^{-1}$ in aqueous (e) 1 M KCl and (f) 1 M LiCl,[8] reprinted with permission from Ref. 8. Copyright 2012 Elsevier. (g) Operando synchrotron XRD patterns of $MnO_2{\cdot}nH_2O$ electrodes during CV cycling in aqueous 1.0 M NaCl. Here, Ti current collector's reflections act as internal standards. The (100) peak shifts to a lower angle during the cathodic scan, indicating lattice expansion, and returns to its original position during the anodic scan. Pseudocapacitance involves the intercalation of cations into the bulk of the oxide structure.[34] Reproduced with permission from Ref. 34. Copyright 2006 The Electrochemical Society. (h) Diagram illustrating various charge storage mechanisms for surface modified Mn-based electrodes as a function of potential. The battery behavior is represented by B, and PC stands for pseudocapacitance. The red ($2.0\,mV\,s^{-1}$) and blue ($100\,mV\,s^{-1}$) lines on the graph show the dQ/dV (current/scan-rate) plots of the Mn-based composite electrode,[28] reprinted with permission from Ref. 28. Copyright 2015 John Wiley and Sons. (i) In-situ Raman spectra of the MnO_2 electrode at different stages of (dis)charging in $1.0\,M\ Na_2SO_4$. The three (ν_1, ν_2, ν_3) peaks correspond to the Mn-O bond stretching vibration of the MnO_6 octahedron. During charging, the ν_1 peak increases with an observed blue shift, indicating Mn-O bond shortening due to the increase in valence state of Mn. In contrast, during discharge, the ν_1 peak weakens with a red shift. Both Raman peaks become sharper at high voltages, attributed to the insertion/extraction process of Na^+,[41] reprinted with permission from Ref. 41. Copyright 2021 Elsevier.

Here, M is the formula weight of the electrode material, F is Faraday's constant $96{,}500\,C\,mol^{-1}$, ΔV is the potential window, and n is the number of reaction electrons. In the case of rutile RuO_2 ($M = 133.07\,g\,mol^{-1}$), $n = 1$ (Ru^{3+}/Ru^{4+}) within the potential range ($\Delta V = 0.2$–$1.2\,V$) can be adopted, so the theoretical capacity can be calculated as $725\,C\,g^{-1}$ ($200\,mAh\,g^{-1}$). Note that this is assuming 100 % utilization (e.g. $Ru^{4+}O_2 + H^+ + e^- \rightarrow HRu^{3+}O_2$) and the contribution from electric double layer (EDL) charging is neglected here. This 100 % reaction is actually not realistic for well crystallize RuO_2 as proton insertion into the rutile-type RuO_2 occurs

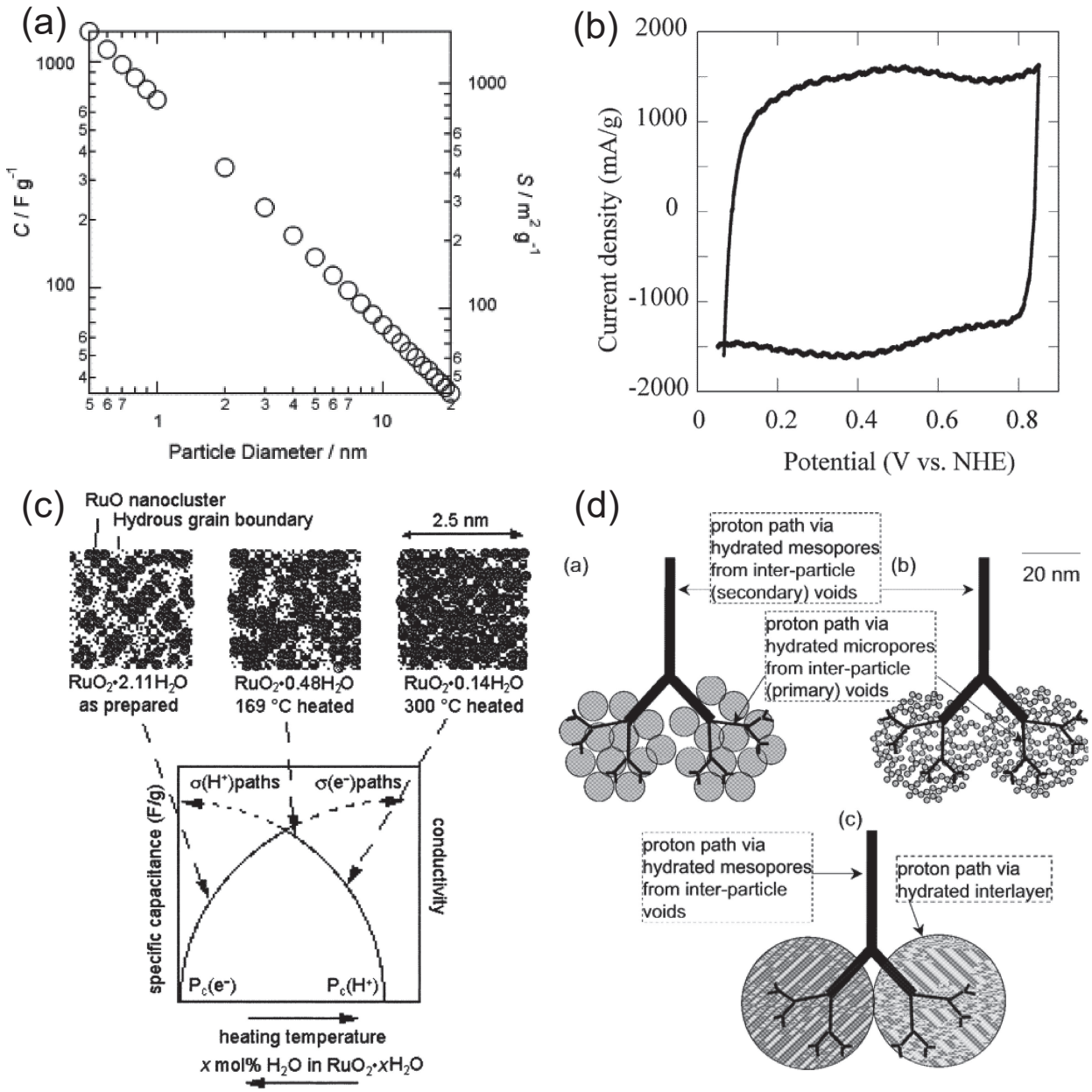

Figure 2. (a) Calculated specific capacitance and the specific surface area as a function of the particle size of RuO_2 using the probe value of 80 μF cm^{-2},[44] reprinted with permission from Ref. 44. Copyright 2006 Elsevier. (b) The featureless 'box-like' CV curve of RuO_2*0.58 H_2O. Measured in 0.5 M H_2SO_4 at a sweep rate of 2 mV s^{-1},[53] reprinted with permission from Ref. 53. Copyright 2002 American Chemical Society. (c) Schematic illustration of the variation of the percolation volumes of the RuO_2 nanocrystals and the hydrous grain boundaries with changes in water content,[53] reprinted with permission from Ref. 53. Copyright 2002 American Chemical Society. (d) A schematic of the fractal trunk-root model for (a) anhydrous RuO_2, (b) hydrous RuO_2, and (c) layered $H_{0.2}RuO_{2.1}$*nH_2O,[55] reprinted with permission from Ref. 55. Copyright 2005 American Chemical Society.

only at <0 V vs RHE and even then, the amount is limited to less than 10 %.[57] Thus, the use of the theoretical capacity of RuO_2 based on the Faraday equation should be taken with care. Nonetheless, this value can be a measure for surface utilization; for example, if RuO_2 has a specific capacity of 180 C g^{-1}, one can say that 25 % of the Ru ions contributed to the redox reactions.

2.3.3 Synthesis, chemical and physical properties

RuO_2 in nanostructured forms such as nanoparticles and nanosheets represent one of the best-known electrode materials for aqueous supercapacitors providing mass specific capacitance ranging from a few hundred to ~1,000 F g^{-1}.[50,58] In addition to the high mass specific capacitance, RuO_2 nanostructures represent materials with significantly improved specific capacitance per volume owing to the high density of 6.97 g cm^{-3} (for rutile-type RuO_2), which is much greater than the density of ~0.5 g cm^{-3} for typical activated carbons. The high gravimetric and volumetric capacitance of RuO_2-based electrodes is appealing, especially where size and weight are a deciding issue such as micro-power sources and other high value-added devices.[59,60]

The specific capacitance, as well as the cycle and rate performance are affected by the various parameters including surface area, crystal structure, water content, etc., which are related to the particle size, preparation procedures and measurement conditions. High-surface area RuO_2 nanoparticles are typically synthesized by low-temperature processing methods including sol-gel reactions,[43,61] hydrothermal treatment,[62] electro-oxidation of Ru metal[63,64] and electrodeposition.[65,66] Heat treatment at relatively low temperatures (150–200 °C) is often necessary to convert all Ru ions to the

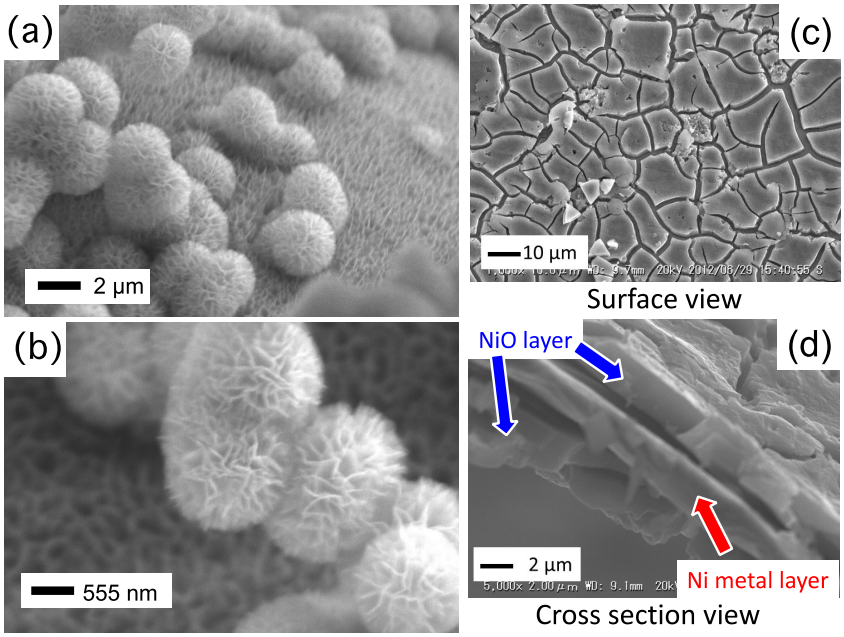

Figure 3. (a and b) SEM images of the NiO electrode prepared with CBD methods in different magnitudes. (c) Top and (d) cross section SEM images of the direct converted NiO electrode,[100] reprinted with permission from Ref. 100. Copyright 2015 Elsevier.

electrochemically stable Ru^{4+} state. As mentioned in the previous section, the high surface area is an important factor since most of the fast redox process occurs at the surface of the material.

Material hybridization by synthesis of RuO_2-MO_x composites (solid solutions or physical mixtures) and A_xRuO_y complex oxides (pyrochlores and perovskites)[67–71] or mixing with various carbonaceous materials[72–75] are classical approaches to increase the utilization of RuO_2. Even a simple physical mixture of acetylene black and sol-gel derived hydrous RuO_2 can drastically improve the rate performance, where the carbon black helps to increase porosity to supply extra pores for electrolyte permeation.[72] The use of buffered solutions allows high specific capacitance at near neutral pH.[76]

High capacitance can also be achieved by using a water swellable layered oxide (~400 F g^{-1}) or by exfoliation of the layered structure into nanosheets (~800 F g^{-1}).[77,78] The exceptionally large capacitance of the layered oxide considering the micrometer size of the particles can be understood by the ability of the interlayer to swell thereby allowing electrolyte permeation into the 2D structure. These 2D materials exhibit unique electrochemical properties with remarkably large contribution from pseudocapacitance (as much as 50 %). Due to the high conductivity and polycationic nature of RuO_2 nanosheets they also can be used as redox active binders.[79]

2.3.4 Charge storage mechanism

RuO_2 nanoparticles with disordered structures exhibit featureless and principally rectangular shaped CV curves in comparison to well-crystalline particles (Fig. 2).[52,53] Ellipsometry, impedance spectroscopy, and RDE studies have revealed that the fast and slow charging modes in porous RuO_2 electrodes can been attributed to the utilization of more accessible, mesoporous surfaces and less accessible, microporous inner-surfaces, respectively.[50,54,80,81] The fast-and slow-charge storage have been ascribed to the charging of the grain surfaces and incorporation of protons into the oxide grains, respectively.

Hydrous RuO_2 nanoparticles enable high capacitance due to the large surface area at the expense of power performance (volcano-plot behavior). X-ray absorption near-edge structure (XANES) and atomic pair-density function (PDF) analysis of synchrotron X-ray scattering measurements revealed that hydrous RuO_2 is composed of disordered rutile-like RuO_2 nanocrystals dispersed by boundaries of structural water.[52,53] A mixed percolation model (parallel electron-proton conduction model), where the rutile-like RuO_2 nanoparticles support electronic conduction and structural water as the boundaries transport protons, was proposed to interpret the volcano-plot behavior (Fig. 3). Based on impedance spectroscopy and X-ray photoelectron spectroscopy (XPS), a trunk-root model (Fig. 4) was proposed to explain the frequency response (power capability).[55,82] Proton conduction within the hydrated micropores between the RuO_2 nanoparticles and the presence of weakly bound physically adsorbed water and strongly bound chemically bound water were suggested to be the determining factors.

2.4 Nickel oxides

EDLCs, which exhibit high power density and long-term cycling characteristics, are being commercialized for applications different from those of rechargeable batteries, which have high energy density but suffer from lower power density and poorer cycling behavior. Due to these limitations, there is interest in developing electrochemical capacitors that utilize various redox reactions for a range of applications. In particular, hybrid capacitors that combine electrodes used in rechargeable batteries with activated carbon electrodes have the potential to realize energy storage devices that combine the energy density of rechargeable batteries with the power density of EDLCs.[83,84]

Various transition metal oxides have been investigated as electrode materials for rechargeable batteries, and nickel oxide (NiO) is known to have a similar composition and reaction mechanism as that demonstrated by the nickel hydroxide ($Ni(OH)_2$) positive electrode in nickel-metal hydride rechargeable batteries which exhibit high capacity and extended cycling properties. The research by Anderson et al. in which nano-size NiO particles were prepared on a nickel metal substrate by the sol-gel method[85] exhibited a capacity of over 200 F g^{-1}. This research has led to the investigation of electrochemical capacitors using various nickel oxide positive electrodes.

Nanosized nickel oxide electrodes have been investigated for use in electrochemical capacitors as these electrodes exhibit very high-rate capability, It should be noted that NiO electrodes do not exhibit pseudo-capacitance even when they are nanosized.[86] Most of the currently studied NiO electrodes for hybrid capacitors clearly show a plateau voltage in the charge-discharge curve, which indicates a

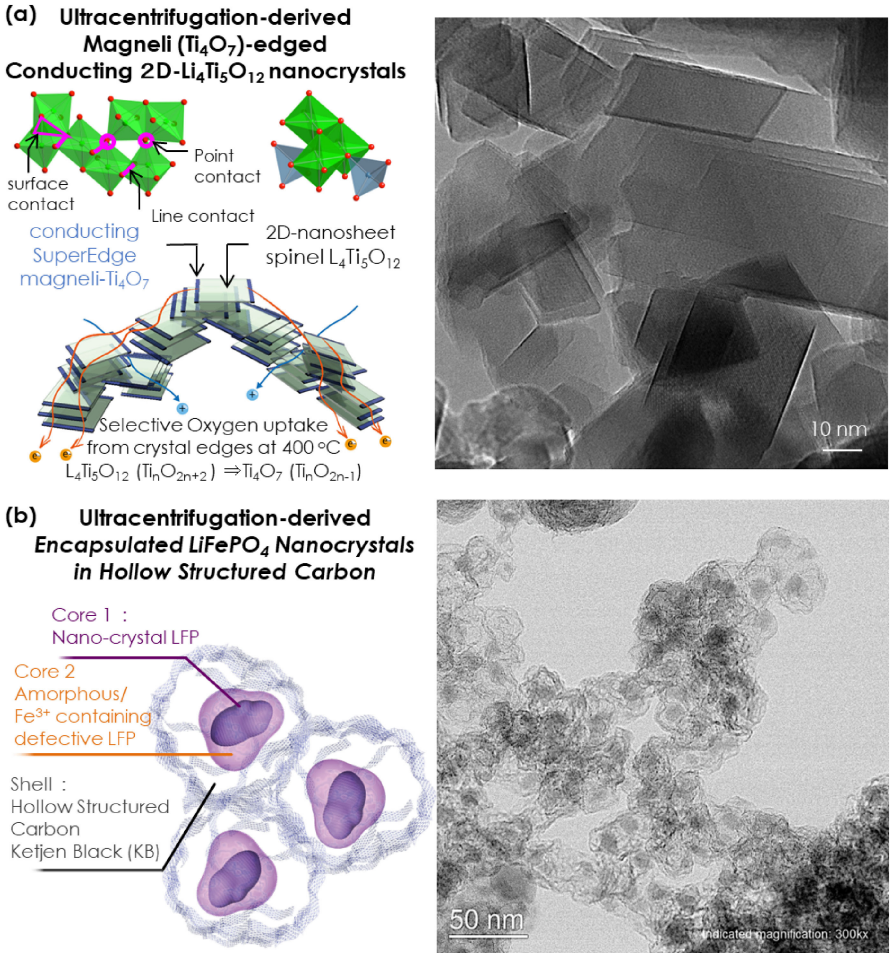

Figure 4. Ultracentrifugation-derived nanocomposites; (a) Magneli (Ti_4O_7)-edged $Li_4Ti_5O_{12}$ nanosheets, and (b) core-shell $LiFePO_4$ nanocomposites.[112] Reproduced with permission from Ref. 112. Copyright 2016 the Royal Society of Chemistry.

battery-like reaction where the diffusion of ions inside the bulk of NiO is the rate-limiting factor. In contrast, for a hybrid capacitor combining NiO electrodes and activated carbon electrodes, the device functions as a capacitor with an activated carbon electrode that exhibits EDLC performance.

The reaction mechanism of NiO electrodes depends on the electrolyte. In neutral and acidic aqueous electrolytes, it follows the following equation.[87]

$$NiO + H_2O \rightleftarrows NiOOH + H^+ + e^- \quad (5)$$

On the other hand, with a basic electrolyte, NiO reacts as follows;[88,89]

$$NiO + OH^- \rightleftarrows NiOOH + e^- \quad (6)$$

Furthermore, since NiO is transformed by hydration to $Ni(OH)_2$ in basic electrolyte, the following reaction mechanism is considered to occur after the initial discharge.

$$Ni(OH)_2 + OH^- \rightleftarrows NiOOH + H_2O + e^- \quad (7)$$

In aqueous Li_2SO_4 solutions, the charge/discharge process proceeds through the insertion of protons as follow;[87]

$$Ni(OH)_2 \rightleftarrows NiOOH + H^+ + e^- \quad (8)$$

Although a limited amount of lithium is also inserted during discharge, there is an indication that charge-discharge proceeds by adsorption and desorption of ions contained in the supporting electrolyte in organic electrolyte.[90] DFT calculations suggest that the adsorption energy of lithium ions on the (111) plane is higher than that on other planes. Therefore, after lithium ions are adsorbed on the (111) plane as the first step, they diffuse to other surface orientations, and after the surface is saturated, diffusion to the bulk interior occurs.

In order for NiO electrodes to achieve the high-rate capability needed for hybrid capacitors, it is important to reduce the ion diffusion distance by reducing the size of electrode active materials. Geometrically, miniaturization can be classified into 0D, 1D, 2D, and 3D.[91,92]

Zero-dimensional microstructure represents NiO nanoparticles. Although nanoparticles exhibit a large surface area, they are easily aggregated during charge/discharge reactions, resulting in a reduction of the electrode surface area. In addition, the relatively low conductivity of NiO results in low electron conductivity and requires a significant amount of conductive additive to ensure sufficient electronic conductivity.[91,92]

Typical 1D microstructures are nanorods and nanowires. These shapes are mainly fabricated by hydrothermal/solvothermal methods and electrospinning. 1D NiO has several advantages including sufficient space for electrolyte to penetrate, which results in good ion diffusion, continuous contact with the current collector and conductive agent, which facilitates utilization of the active material. On the other hand, the energy density per volume may be low due to its small density.[93,94]

2D microstructures are generally in the form of nanoplatelet structures. Such structures are realized by microwave irradiation methods, precipitation methods, and chemical bath deposition (CBD) methods.[95] The CBD method is a unique approach used for the preparation of NiO electrodes. The current collector was simply immersed in a bath of $Ni(OH)_2$ solution and mixed with

potassium peroxodisulfate solution for 15 minutes. Figures 3a and 3b shows the SEM image of a NiO electrode fabricated by the CBD method. Flower-like NiO layers were modified on a nickel foam substrate. The flower-like structure avoided restacking of the 2D nanomaterials and achieved long cycle life. Nanoplatelet structures can achieve a higher surface area in a smaller volume. On the other hand, a continuous platelet structure may impede the path of ion diffusion or the penetration of electrolyte.[96,97]

Three-dimensional microstructures are porous structures in which micropores or regularly arranged pores exist in the bulk material. Such structures are fabricated by hydrothermal/solvothermal or template-assisted methods, etc. In 3D microstructures, it is possible to control the surface area per volume and ion diffusion by controlling the diameter and volume of pores.[98,99] NiO electrodes are generally fabricated using nickel foam as a metal current collector. Although nickel foam has a large surface area, its weight per area is typically heavier than the active material. This is because active materials for capacitors require high ion diffusion, making it difficult to load active materials at high density as occurs in rechargeable batteries. To solve this problem, electrodes were fabricated by directly converting the surface of a thin nickel foil to NiO. Since nickel is not a valve metal, it is generally difficult to form a thick oxide layer on the surface by anodic oxidation, but by using nickel fluoride, it is possible to create a NiO layer with a thickness of 2–3 microns. By applying this technique to a 10 micrometers thick nickel foil, it is possible to fabricate a structure in which a 3 to 4 micrometer thick current collector layer made of metallic nickel is sandwiched by a 2 to 3 micrometer thick NiO layer (Figs. 3c and 3d).[100] Such NiO positive electrodes are widely used in electrochemical capacitors.

3. Non-oxides and Emerging Materials

3.1 Complex materials

Supercapacitors have emerged as pivotal energy conversion and storage systems in contemporary renewable and sustainable nanotechnology, providing a cost-effective and environmentally friendly solution.[101] Their unique material properties, characterized by exceptional high-power capabilities and longevity, distinguish them from conventional batteries, rendering them versatile for a wide range of applications. Their attractive features, including extended cycle life and high-power capabilities, make them particularly appealing for advanced hybrid configurations, catering to both mobile and stationary needs across diverse sectors. The pursuit of shaping the next generation of energy technologies drives the development of composite materials, which integrate elements such as nanocarbon and metal oxides to enhance electrochemical performance. Material selection plays a crucial role in optimizing supercapacitors, as different materials used in electrodes and electrolytes significantly impact functionality and characteristics, especially in terms of electrochemical and electrical properties.

Innovative techniques such as "Ultracentrifugation"[102,103] and "Spray-Dry Quenching"[104] are instrumental in engineering nanoarchitecture electrode materials. Ultracentrifugation, for instance, facilitates the rapid generation of nano-sized precursors followed by instantaneous post-heat treatment, resulting in optimized "nano-nano composites" capable of delivering energy at the highest sustained power performance across varying temperatures and rates. This method enhances the rate of most of the Li-insertion compounds, making them viable alternatives for enhanced hybrid supercapacitors.

A good example of the use of Ultracentrifugation is when it produces nanosheets composed of Ti_4O_7-Edged $Li_4Ti_5O_{12}$ nanosheets, which demonstrates ultrafast electrochemistry in a composite nanoarchitecture material (Fig. 4a). This unique material configuration exhibits inherently high electrical conductivity, making it suitable for commercialized "NanoHybrid Capacitors (NHC)" configured as UC-$Li_4Ti_5O_{12}$//Activated Carbon.[102] Ultracentrifugation has also been successfully applied to enhance various lithium intercalation materials such as $Li_4Ti_5O_{12}$,[102,105] SnO_2,[106] TiO_2(B),[107] Li_3VO_4,[104,108–111] $LiFePO_4$,[112–115] and $Li_3V_2(PO_4)_3$.[116–118] For example, the development of core-shell $LiFePO_4$ nanocomposites synthesized via Ultracentrifugation enables ultrafast symmetric charge-discharge rates, overcoming inherent diffusion limitations (Fig. 4b).[112] This advancement presents new opportunities for designing hybrid supercapacitors with unprecedented performance.

The "SuperRedox Capacitor (SRC)," introduced as the 3rd-generation supercapacitor, adopts ultrafast electrodes fabricated via ultracentrifugation for both positive and negative terminals. Structurally akin to batteries, the SRC is aptly dubbed the "Super Battery." Notably, an investigation into the SRC(UC-Li_3VO_4//UC-$Li_3V_2(PO_4)_3$) configuration yielded unprecedented performance, boasting an energy density 5.7 times higher than that of EDLCs operating at 3.5 V.[119] $Li_3V_2(PO_4)_3$ emerges as a prominent candidate for positive SRC electrodes due to its exceptional high-rate performance. Ultracentrifugation-derived UC-$Li_3V_2(PO_4)_3$/CNT composites facilitate high C-rate operation, achieving 96 mAh g^{-1} @300C.[116] However, full cells based on $Li_3V_2(PO_4)_3$ experience capacity degradation during cycling, attributed to electrolyte decomposition on the negative electrode resulting from minute quantities of vanadium dissolution.[120,121] Efforts to mitigate this issue involve substituting vanadium with various elements, leading to the composition of $Li_{2.9}V_{1.9}Ti_{0.1}(PO_4)_3$, which notably enhances capacity retention to 88.6 % after 10,000 cycles.[117] For the negative electrode, a novel double capsule structure of nanocrystalline lithium superionic conductor (LISICON)-type γ-$Li_{3.2}V_{0.8}Si_{0.2}O_4$ has been developed using a straightforward spray-drying method.[104] This structure exhibits a highly efficient network of electrons/ions, featuring graphitic carbon on the surface of γ-$Li_{3.2}V_{0.8}Si_{0.2}O_4$ nanoparticles and an amorphous carbon network among them (Fig. 5). Consequently, this nanoarchitecture facilitates outstandingly fast discharge performance.

Innovative techniques such as "Ultracentrifugation" and "Spray-Dry Synthesis" are leveraged to engineer nanoarchitecture electrode materials, leading to significantly improved performance and safety standards. These advancements propel the evolution of supercapacitors towards greater efficiency and reliability in energy storage applications.

3.2 Metal-organic frameworks

Significant progress has been made in the field of organic-based electrode materials for energy storage in recent years. This research area started with the discovery of electrically conductive polymers in which the doping of anions or cations were shown to enhance conductivity in electrode materials.[122] Scientists also investigated organic molecular materials utilizing oxygen or sulfur redox reactions to further increase energy storage. Notable examples of materials include those that are quinone-based, radical-based, or have disulfide-based functions.[123] More recent studies have shifted to MOFs, a type of material composed of organic molecules and metal ions that form self-assembled structures with pore networks.[124] MOFs are known for their gas adsorption and separator applications, and some of these materials exhibit electrical activity and intercalation reactions, making them interesting candidates for electrode materials.[125,126] The self-assembly in MOFs can solve several problems which limit conventional organic electrode materials. This includes such as physical properties related to electronic conduction, chemical stabilities related to electrolyte dissolution during charging and discharging,[127] and low density due to polymerization.[128]

A number of recent studies have focused on the fast-charging performance of MOF electrodes for lithium-based capacitor applications and establishing the relationship between the crystal structure of MOFs and their electrochemical properties. A set of

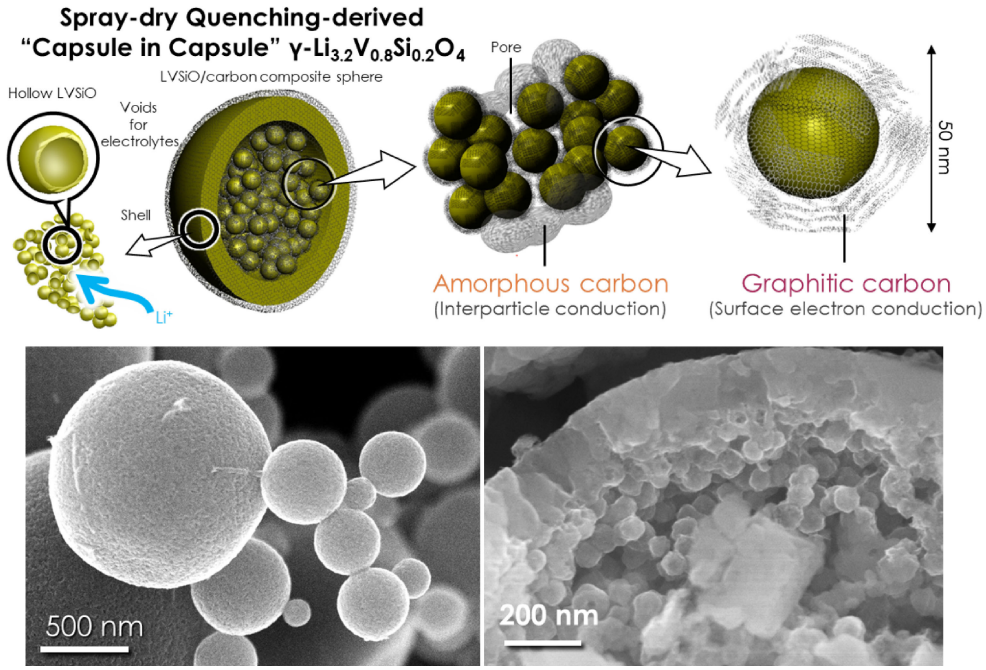

Figure 5. Spray-dry quenching-derived double capsuled γ-$Li_{3.2}V_{0.8}Si_{0.2}O_4$ nanocomposites, featuring graphitic carbon on the surface of γ-$Li_{3.2}V_{0.8}Si_{0.2}O_4$ nanoparticles and an amorphous carbon network among them.[104] Reprinted with permission from Ref. 104. Copyright 2023 the Royal Society of Chemistry.

framework materials composed of Li^+ ions and aromatic dicarboxylates forms an organic–inorganic layered structure consisting of aromatic π-stacks and a tetrahedral LiO_4 network of carboxylate groups (Fig. 6a).[129,130] The material shows reversible Li intercalation via carboxylate anion redox inside self-assembled structures at the potential range from 0.5 V (vs. Li/Li^+) to 1.0 V. Thus, these materials are classified as Li-intercalated MOFs (iMOFs).[131] The operating potential, reversible capacity, and charge–discharge polarization depend on the type of organic structures (Fig. 6b). For example, terephthalate dilithium (Ph), one of the first reported electrode materials,[132] exhibits approximately half of its theoretical capacity because of its high polarization which would lead to high resistance in a practical battery electrode.[131] 2,6-Naphthalene dicarboxylate dilithium (Naph) exhibits high capacity utilization that is almost equal to the theoretical capacity of the practical battery electrode,[131,133] but it also exhibits relatively high polarization and internal resistance.[134] 4,4′-Biphenyl dicarboxylate dilithium (Bph) also exhibits appealing theoretical capacity and low internal resistance.[134,135] As shown in Fig. 6c, the operating potential of iMOF electrodes extends between the potentials of graphite carbon (0.05 V) and $Li_4Ti_5O_{12}$ (1.55 V). This intermediate operating potential in iMOF electrodes can be expected to overcome both the internal short-circuit risk due to Li dendrite in graphite carbon and the low cell voltage in $Li_4Ti_5O_{12}$. In addition, the ability to use Al instead of Cu as a current collector allows the design of high-voltage bipolar batteries.[131] In the case of constructing non-aqueous Li-ion capacitors by combining iMOF negative electrodes with activated carbon positive electrodes, a high energy density design can be achieved.[134,136] This is due to the reduction of Li dendrites caused by the operating potential, which increases the utilization of the negative electrode capacity.

Detailed crystal structure analysis during Li intercalation shows that the volume change during charge-discharge is 0.33 % (Fig. 6d),[131] which is very small compared to nearly all inorganic electrode materials. This low level is expected to suppress mechanical electrode degradation due to volume change. Analysis of the crystal structure change and Li diffusion behavior during charge-discharge revealed that the phase transition mechanism during the reaction is a two-phase coexistence reaction for Naph[131] and a solid solution reaction for Bph.[135] Although iMOF is initially a white powder, it turns black when doped with Li^+ ions (Fig. 6e).[137] Computations indicate that Li^+ ion doping leads to hopping electron conduction at the π-stacking in the aromatic unit, resulting in a change from insulating to electron conducting (Fig. 6f).

To achieve fast charging with iMOF electrodes, hollow particles consisting of nano-sized thin flakes were synthesized using spray-drying (inset in Fig. 6g).[138] This method takes advantage of iMOF's ability to easily crystallize at low temperatures of around 200 °C. These particles are crushed during electrode fabrication to form an electrode structure in which the flakes are uniformly dispersed, resulting in much lower internal resistance as determined by electrochemical impedance spectroscopy,[139,140] as compared to existing electrode materials (Fig. 6g).[138] Although Bph exhibits the lowest resistance in a single aromatic frame, it leads to relatively large charge–discharge polarization at the completion of Li deintercalation.[134,141] Therefore, iMOFs composed of heterogeneous organic structures with fast-charging performance were synthesized using a combination of optimal compositions predicted by machine learning[142] and the use of spray-dry synthesis (Fig. 7a).[143] Optimally composed heterogeneous iMOF samples exhibit strain within the crystal structure, which improves Li diffusivity within the crystal by suppressing bending vibrations that disrupt planarity and affect π-electron conjugation in aromatics.[143] This results in significant improvements in fast charging performance, as shown in Figs. 7b and 7c. This sample exhibits no change in charge-discharge polarization across a wide capacity range, which enhances the utilization of the negative electrode in Li-ion capacitors and improves their high-temperature self-discharge characteristics.[143] There are two other features which make iMOFs a promising research direction. One is the low-temperature crystallization of these electrode materials which reduces energy consumption during fabrication compared to existing materials that require high-temperature processing.[143] A second advantage is the low risk of resource depletion that makes MOF electrode materials appealing for sustainable production.

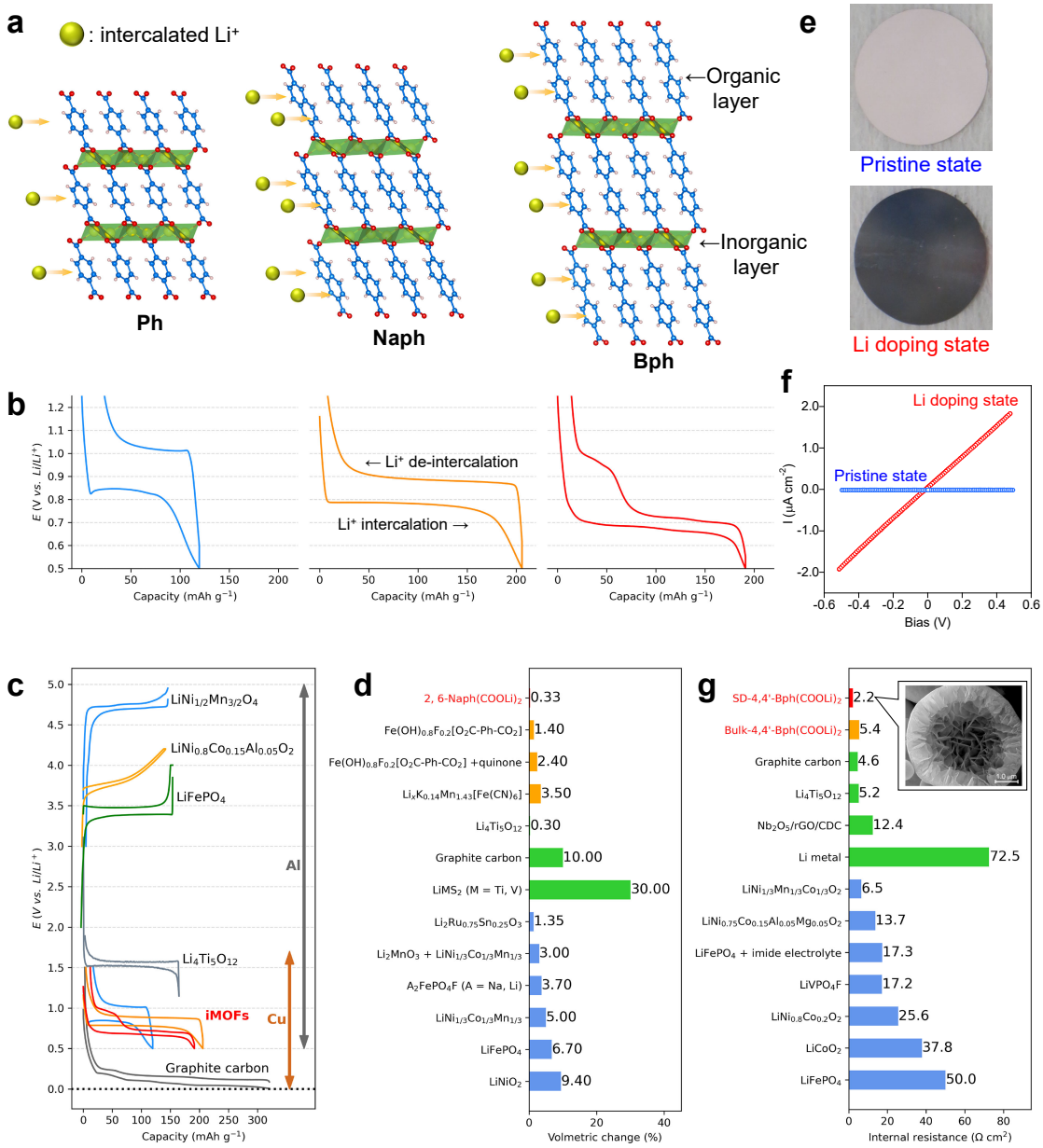

Figure 6. (a) Images of crystal structures and Li intercalation reaction in the series of aromatic dicarboxylate dilithium, and (b) their charge and discharge potential profiles in Li|iMOF cells. (c) Comparison of the electrode charge and discharge profiles of the iMOFs with those of other possible positive and negative intercalation electrodes with the effective potential ranges of Al and Cu current collectors, and (d) comparison of the change in the volume during intercalation reaction,[131] reprinted with permission from Ref. 131. Copyright 2014 John Wiley and Sons. (e) Photographs of 2,6-Naph(COOLi)$_2$ electrode without conductive carbon before (top) and after (bottom) Li doping, and (f) comparison of *I-V* curves,[137] reprinted with permission from Ref. 137. Copyright 2017 Authors CC BY-NC 4.0. (g) Comparison of the internal resistance through impedance measurement using symmetric cell. Inset: SEM image of 4,4′-Bph(COOLi)$_2$ powders via spray-dry synthesis,[138] reprinted with permission from Ref. 138. Copyright 2021 American Chemical Society.

4. Nanosize Effects and 2D Materials

4.1 Zero-dimensional nanomaterials

The size reduction of redox-active materials can provide multiple effects on the performance of energy storage systems, especially for the electrochemical capacitors and high-power devices. First, the exposed surface area or the so-called specific surface area of electrode materials is linearly increased with decreasing the particle size, which leads to an increase in the double-layer capacitance. Second, the surface-to-volume ratio of electroactive materials is also increased with decreasing the particle size, commonly promoting the utilization and specific capacitance of active materials due to the enhanced exposure to electrolyte. This effect is especially important for pseudocapacitive materials with their charge storage reactions occurring at the electroactive materials surface or near surface, such as anhydrous RuO_2[144] and amorphous MnO_2.[145] Third, the Faradaic charge-transfer reactions of battery-type materials generally involve ion diffusion during the redox transitions. The reduction in particle size can shorten the diffusion length of ions and increase the power performance of the resulting electrodes. Fourth, when the solid-state diffusion distance of battery-type materials is located within the "thin-layer" diffusion domain, ion diffusion transport is believed to involve the entire volume of the active materials (similar to the thin-layer diffusion phenomenon in liquid media). Accordingly, there will be no semi-infinite diffusion limitations, making the simple linear dependence between the voltammetric current density and scan rate of CV/linear sweep voltammetry, leading to the ideal capacitor responses. This phenomenon has been described as the

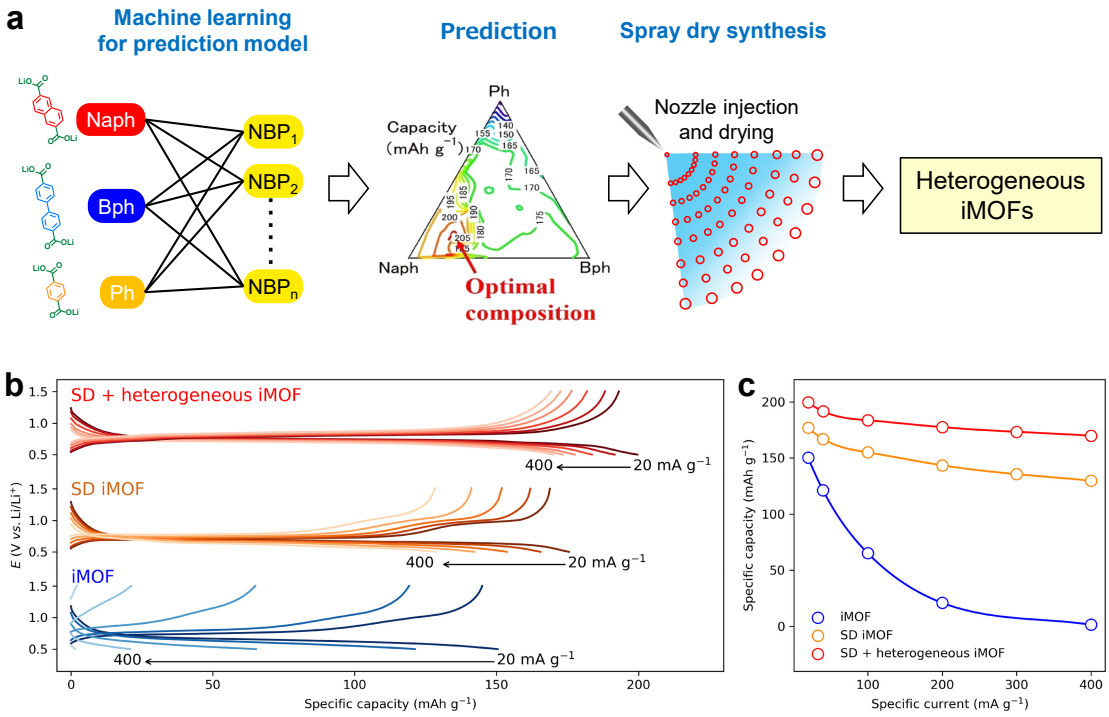

Figure 7. (a) A concept for the creation of heterogeneous iMOF materials. (b) Charge and discharge potential profiles in Li|iMOF cells at different currents from 20 mA g^{-1} to 400 mA g^{-1}, and (c) capacity retention plots at each specific current,[138,143] reprinted with permission from Ref. 138. Copyright 2021 American Chemical Society. Also reprinted with permission from Ref. 143. Copyright 2023 Aurhors, CC BY 4.0.

"extrinsic" pseudocapacitive behavior of nanosized T-Nb_2O_5, initially demonstrated by Dunn et al.,[146] very different from the "intrinsic" pseudocapacitive materials with a confined superficial redox layer. Similar phenomena have been found for various redox-active materials, such as α-MoO_3,[147] TiO_2 (B),[148] $LiCoO_2$,[149] etc., somewhat confusing the definition of pseudocapacitive materials[150] although the hybrid capacitors exactly consist of one capacitor-like electrode and one battery-type electrode to further enhance the device energy density.

In fact, certain nonporous carbon materials with an amorphous microstructure and/or other microstructures also show pseudocapacitive responses involving both anion and cation intercalation/deintercalation mechanisms in organic electrolytes when a proper electrochemical activation process has been applied to create the sub-nanometer space for ion storage. These special carbon materials include alkali-modified soft carbon,[151] reduced graphene oxide,[152] and expanded mesocarbon microbead.[153] For example, Morita et al.[154] investigated the capacitive behavior of alkali-treated soft carbon with a relatively small specific surface area (ca. 50 $m^2 g^{-1}$) for anion storage in organic electrolytes. The use of a hard carbon negative electrode with Li-ion electrolytes makes the cell into a 4.6 V hybrid capacitor with an extremely high-volumetic energy density. The ion storage in the created confined sub-nanometer/nanometer space of such nonporous carbons exhibits intrinsic pseudo-capacitive characteristics.

From the high value for Li-ion storage capacity, and the high-rate characteristics, Li-ion intercalation/deintercalation behavior on the surface or near surface of soft carbon and hard carbon enable them to be considered as pseudocapacitive materials (see Fig. 8). It should be noted that the initial coulombic efficiency of both redox-active materials is relatively low as these materials need the pre-lithiation step for constructing Li-ion capacitors. The hard carbon behavior in Fig. 8a shows two intrinsic regions for Li-ion storage: the slope and plateau regions. The unusual plateau region has been revealed to be a micropore filling mechanism with pore size <0.7 nm.[155] The commonly observed slope region is regarded as the adsorption of Li ions on the nonporous hard carbon (i.e., $Li^+ + e = Li$; also valid for soft carbon) because of its high-rate characteristics from a comparison of all curves shown in Fig. 8a. This Li-ion storage step on the hard carbon surface is not attributable to the double-layer process since the reversible capacity of Li-ion storage is as high as 200 mAh g^{-1} and the open pore surface area of hard carbon is very low (<5 $m^2 g^{-1}$). However, if the surface redox reactions are regarded as the underpotential deposition (UPD) of Li, the Gibbs free energy for this UPD reaction will be as high as 1.06 eV per Li ad-atom, which is too large to be acceptable because the slope region commences at ~1.1 V (vs. Li^+/Li). Consequently, this ion storage process on the hard carbon and soft carbon surface (i.e., the slope region) is considered to be superficial Li-ion intercalation/deintercalation process at the disordered nanosized graphene layers, giving rise to an intrinsic pseudocapacitive characteristic similar to the cation intercalated into randomly distributed nano-sized layers of δ-MnO_2.[156]

4.2 Two-dimensional nanomaterials

MXenes are an emerging family of capacitive electrode materials, which were first synthesized by the research group led by Gogotsi and Barsoum.[157,158] At the early stage of their development, layered MAX phases ($M_{n+1}AX_n$, M = Ti, V, Cr, Nb, Mo, etc.; A = Al, Sn, Ga, etc.; X = C, N, B; n = 1–3) were treated with etching solutions such as hydrofluoric acid to remove A layers for the synthesis of MXenes. Lewis bases (F^-, Cl^-, OH^-, etc.) in the etching solution are nucleophilically attached on remaining $M_{n+1}X_n$ layers as surface termination groups, thus the general formula of MXenes is $M_{n+1}X_nT_x$ (T = F, O, OH, Cl, etc.) (Fig. 9a). After a decade of effort, MXenes are synthesized by (i) a solution-etching method,[159] (ii) a molten-salt method,[160,161] (iii) a direct method and (iv) a chemical vapor deposition method.[162] The composition of the surface termination groups can be controlled by synthetic conditions. For example, the solution etching using the mixture of lithium fluoride and hydrochloric acid gives T = F, O, OH, and Cl[163] while the molten-salt etching using $CdCl_2$ or $CdBr_2$

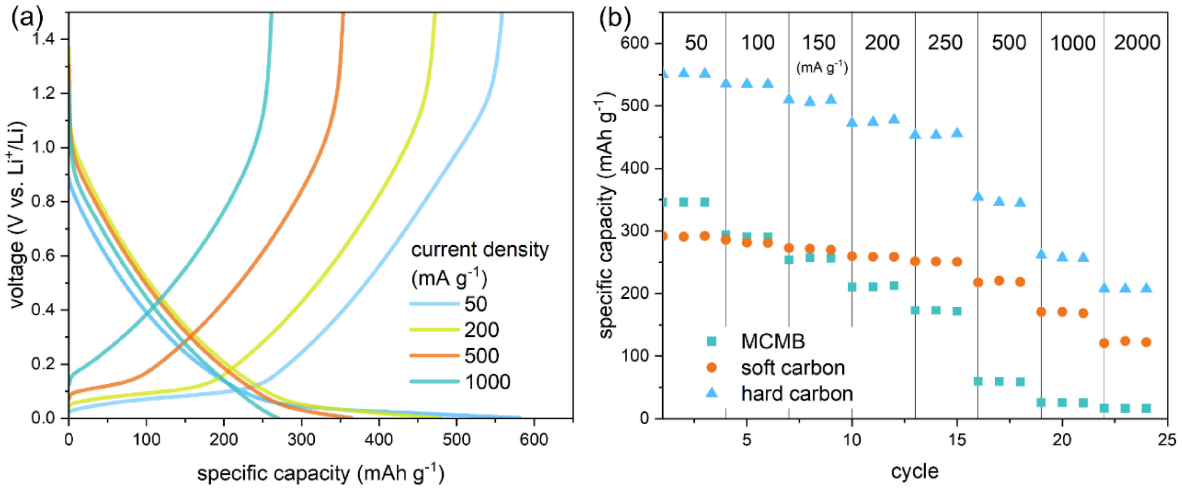

Figure 8. (a) The lithiation and de-lithiation curves of hard carbon synthesized by means of the method at (1) 50, (2) 200, (3) 500, (4) 1000 mA g^{-1}, and (b) the specific capacity of (1) MCMB, (2) soft carbon, and (3) hard carbon at various C rates for Li-ion storage in 1 M $LiPF_6$ in EC/EMC/DMC = 1/1/1(v/v),[155] Reproduced with permission from Ref. 155. Copyright 2023 the Royal Society of Chemistry.

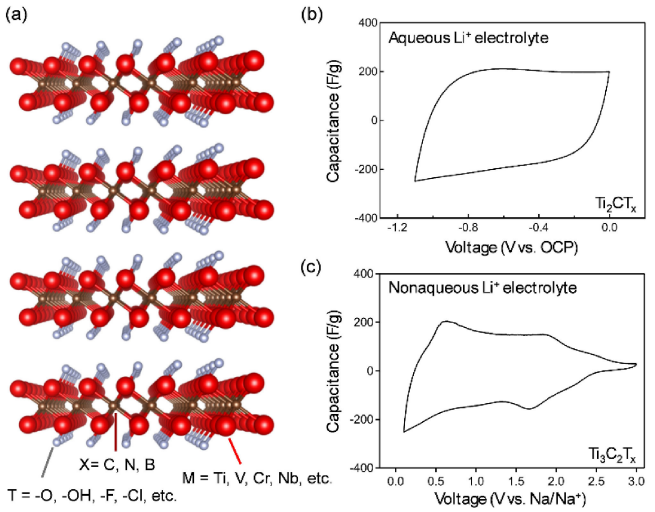

Figure 9. (a) Schematic illustration of MXene $M_{n+1}X_nT_x$. (b) CV curve for MXene Ti_2CT_x in a concentrated aqueous Li^+ electrolyte at a scan rate of 0.5 mV s^{-1},[168] reprinted with permission from Ref. 168. Copyright 2019 American Chemical Society. (c) CV curve for MXene $Ti_3C_2T_x$ in nonaqueous Na^+ electrolyte at a scan rate of 0.2 mV s^{-1},[179] reprinted with permission from Ref. 179. Copyright 2016 American Chemical Society.

gives T = Cl or Br, respectively.[161] Furthermore, post treatment using ammonium persulfate (APS) solution transforms Cl termination to O/OH termination.[161] Importantly, the surface termination groups T as well as the chemical composition M and X strongly influence electrochemical properties.[164,165] MXenes can be delaminated to nanosheets, which also affects electrochemical properties.[166,167]

MXene electrodes in aqueous electrolytes exhibit a capacitive behavior (Fig. 9b).[168] Although their specific capacitance depends on various experimental conditions, machine-learning assisted data clarified that it generally increases in the order of $H^+ > Li^+ > Na^+ > K^+$.[169,170] One possible explanation is the increase in orbital hybridization between alkali cation and surface termination groups to give larger charge transfer (pseudocapacitance or quantum capacitance).[171] Another explanation is the change in the dielectric response (overscreening) of a hydration layer confined in interlayer space.[169] Delamination of MXenes frequently improves the rate capability owing to faster ion migration in expanded interlayer space while the larger surface area of delaminated MXene contributes to larger capacitance.[166,172] The influence of the surface termination groups on electrochemical properties has yet to be fully understood. For example, molten-salt synthesized MXenes show no electrochemical activity in aqueous electrolytes[173] while the transformation of Cl termination to O/OH termination using the APS solution significantly increases the capacitance.[174] Density functional theory calculations combined with reference interaction site model calculations suggested that the specific capacitance with an aqueous K^+ electrolyte increases in the order of I > Br > Cl > F due to the decrease in the electric double-layer thickness.[175]

MXene electrodes in nonaqueous electrolytes exhibit complex behavior due to the formation of solid-electrolyte interphase. The specific capacity increases in the order of $Li^+ > Na^+ > K^+$ presumably because smaller cations can be accumulated more densely in the interlayer space.[176–178] Note that the electric double-layer capacitance in nonaqueous electrolytes is negligible because the intercalation of desolvated ion mainly gives rise to battery-type reaction (large charge transfer) (Fig. 9c).[179] However, polar solvents such as dimethyl sulfoxide co-intercalate to decrease the specific capacity.[180] From a practical application viewpoint, MXene electrodes show a large irreversible capacity upon the first charge and hence low initial Coulombic efficiency of typically <70 %. Most likely, the irreversible reactions of defects[181] and/or surface termination groups in addition to electrolyte decomposition (SEI formation) occur. Although many papers have reported that implementing redox-active elements such as Sn achieves the large specific capacity of >600 mAh g^{-1},[182] such decoration further degrades initial Coulombic efficiency, which would severely impede their application in EES devices. Thus, control of defects and surface termination groups are important steps towards the development of practical MXene electrodes.

5. Electrode-electrolyte Interfaces

5.1 Halide systems

EES can be realised by either EDL or Faradaic (i.e. charge transfer) processes which can follow either a Nernstian or a pseudocapacitive mechanism, or a combination of the two.[183,184] The Nernstian storage process is governed, at least broadly considering kinetic complications, by the Nernst equation and is commonplace in rechargeable batteries. It causes peaks on CVs and plateaus on galvanostatic charge-discharge curves (GCDs). How-

ever, in the context of supercapacitor research, pseudocapacitance corresponds to the same or comparable performance features as EDL charge/discharge that presents typically rectangular CVs and triangular GCDs.

Historically, the concept of pseudocapacitance was used as a measure of electro-adsorption which is Nernstian in nature.[185,186] As a result, the pseudocapacitance attributed to electro-adsorption (or more recently Nernstian storage) does not show rectangular CVs or triangular GCDs. Further, such pseudocapacitance offers a non-linear relationship between the charge stored and the applied electrode potential, which leads to the term nonlinear pseudocapacitance. In contrast, the rectangular CV corresponds to pseudocapacitance that offers a linear charge-potential relation and is consequently termed as linear pseudocapacitance.[187] The fundamental difference between the two is that materials of linear pseudocapacitance can be described by a single capacitance value, but their non-linear counterparts cannot.

Unfortunately, the literature on pseudocapacitance has remained confusing[16,187,188] and it is necessary to describe linear pseudocapacitance as Faradaic capacitance or redox capacitance. It can help not only avoid unnecessary confusion with those literatures claiming pseudocapacitance for Nernstian or battery electrode materials, but also remove any ambiguity because Faradaic capacitance is not a pseudo-property. Instead, it is an intrinsic nature of most, if not all, semi-conductor materials in which zone-delocalisation of valence electrons occurs.[189] This understanding agrees well with the capacitive properties of properly doped semi-conducting metal oxides and sulfides, and conjugated conducting polymers. On the other hand, materials with non-linear pseudocapacitance store charge follow the Nernstian mechanism and hence are the same as battery electrode materials. In other words, non-linear pseudocapacitance fits well with battery electrochemistry and should be distinguished from supercapacitors.

Nevertheless, it should be pointed out that both linear and nonlinear pseudocapacitances or Faradaic and Nernstian charge storage mechanisms can be effectively employed in EES devices. The selection of which mechanism is responsible is less important than whether optimal performance of the device is achieved. In line with this principle, research and commercial efforts have been made to combine any two or even all three of the EDL, Faradaic and Nernstian charge storage mechanisms into one device. Examples include (1) asymmetrical supercapacitors that combine EDL and Faradaic capacitances, (2) lithium or other metal ion capacitors and, more generically, (3) "supercapatteries" that merge capacitive and Nernstian storage mechanisms. Figure 10 illustrates schematically these charge storage mechanisms and their relationships and possible combinations. (NB: The terms of metal ion capacitor and hybrid supercapacitor may lead to the impression that such devices belong to the capacitor or supercapacitor categories, but they are not.)

Such combinations do not necessarily guarantee a better hybrid in terms of performance, cost, safety and sustainability. A successful

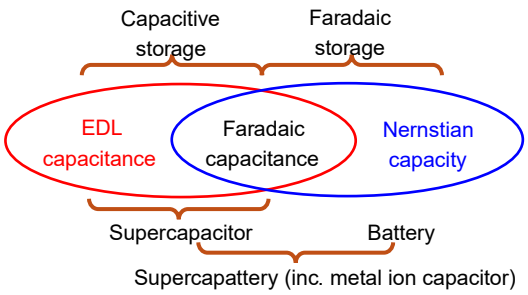

Figure 10. Relationship between different electrochemical charge storage mechanisms and their possible combinations.

combination must start from careful considerations of both theoretical and practical feasibilities. Theoretical analyses can be applied well to predict the specific charge capacity and maximum cell voltage, and hence the energy storage capacity. However, power capability and cycle life are, to a large extent, engineering issues in relation to materials, electrode and cell structures and dependent on fabrication and device operation.

Among the various reported and successful combinations is a technically simple and hence cheaper but highly effective approach: the use of redox electrolytes in supercapacitors.[189–193] Because redox reactions contribute to enhancing the charge storage capacity, the mechanism is no longer purely capacitive. Consequently, supercapacitors with redox electrolytes are in fact supercapatteries.[194]

Various redox active molecules and ions have been tested in the electrolytes of supercapacitors with e.g. porous carbon electrodes. An imperative property of the added redox species is that both of its oxidised and reduced forms can remain in the electrode via a certain mechanism, such as chemical or physical adsorption or electrostatic attraction. Otherwise, shuttling of the redox species between the two electrodes may occur unless a suitable separating membrane is used.

Activated carbons are the best electrode materials in this case because they offer various pore structures and oxygen containing groups on their internal wall surfaces, offering favourable reactive sites for the adsorption of the redox active species. Another favourable mechanism for the retention of the redox species in the porous electrode is to select those whose oxidised and reduced forms have the same type of charge. A good example is the reversible electro-oxidation of iodide (I^-) to tri-iodide (I_3^-) in an aqueous electrolyte. Similar electrode reactions occur to with other halide ions (X^-) as expressed by reactions (9) and (10).

$$2X^- \rightleftharpoons X_2 + 2e \quad (X = I,\ Br,\ Cl) \tag{9}$$

$$X^- + X_2 \rightleftharpoons X_3^- \tag{10}$$

The standard potential of reaction (9) is 0.54, 1.06 and 1.36 V for X_2 being I_2 (solid), Br_2 (liquid) and Cl_2 (gas), respectively. The occurrence of reaction (10) shifts the potential negatively with the magnitude of change depending on the nature and composition of the solution. For example, in aqueous solutions, both I_3^- and Br_3^- can form via reaction (9) which however does not occur to Cl^- whose anodic oxidation produces Cl_2 gas that escapes from the solution. In other words, reaction (10) either does not occur or is insignificant if present.

Interestingly, a study of the energetics of the trihalide ions has revealed the stability order of $I_3^- > Br_3^- > Cl_3^-$ in water but the reverse is true in acetonitrile.[195] Further, the formation of the trichloride ion (Cl_3^-) was found to lead to the absence of Cl_2 gas evolution on a platinum (Pt) anode during electrolysis of 1-butyl-3-methylimidazolium hexafluorophosphate ([BMIM]PF_6) with high concentrations of 1-butyl-3-methylimidazolium chloride ([BMIM]Cl).[196]

Figures 11a and 11b show the CVs of a Pt micro-disk electrode recorded in [BMIM]PF_6 containing different chloride and bromide salts.[197] It can be seen that in all cases both oxidation and reduction current peaks appear on the CVs, although the reduction peaks are noticeably smaller than the oxidation ones. This observation reflects not only viable kinetic contributions but also the expected effect of the micro-disk electrode. It can also be noted that a large single peak results from Cl^- oxidation, but two peaks are recorded for Br^- oxidation. Further detailed electrochemical analyses indicate the second peak being highly likely from the oxidation of Br_3^- to Br_2 according to reaction (11). This finding actually agrees with the claim that Br_3^- is less stable than Cl_3^- in acetonitrile.[195]

$$2Br_3^- \rightleftharpoons 3Br_2 + 2e \tag{11}$$

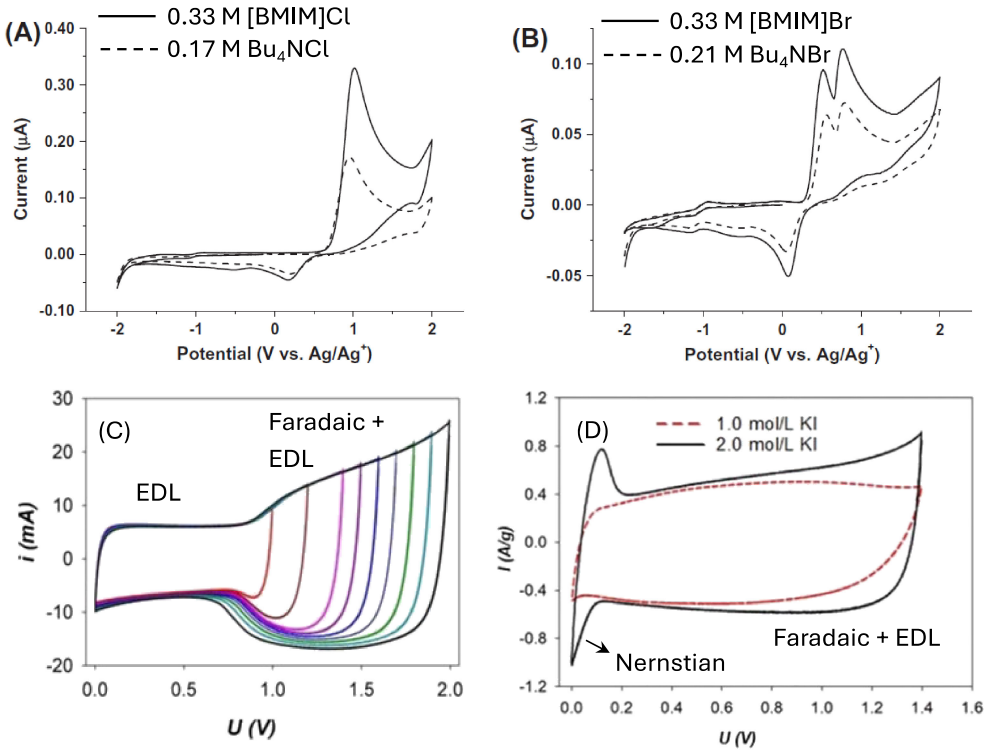

Figure 11. (A, B) CVs of a Pt-micro-disc electrode (diameter: 100 μm) in $[BMIM]PF_6$ containing (A) chloride and (B) bromide salts at indicated concentrations. Scan rate 50 mV s^{-1}.[197] Reprinted with permission from Ref. 197. Copyright 2013 Elsevier. (C, D) CVs of a symmetrical cell of activated carbon containing an aqueous electrolyte of (C) 1.0 M KBr and (D) 1.0 M (red dashed line) and 2.0 M (black solid line) KI. Scan rate = 5.0 mV s^{-1}.[194] Reproduced with permission from Ref. 194. Copyright 2018 Aurhors, CC BY 4.0.

The higher stability of Cl_3^-, together with the more positive potential for Cl^- oxidation, make the Cl^-/Cl_3^- couple a favourable choice for enhancing the charge storage performance of a positive electrode of porous carbon via electrostatic adsorption.

In addition, a number of chloride salts of "soft metals", e.g. $FeCl_3$ and $AlCl_3$, are able to form intercalation compounds with graphitic carbons. This property has been employed in the relatively new ionic liquid based aluminium ion battery[198,199] in which the graphite positive electrode is the host for the fast de-/intercalation of the anionic $AlCl_4^-$ complex according to reaction (12).

$$C_n + AlCl_4^- \rightleftharpoons C_n[AlCl_4] + e \quad (12)$$

This reaction is expected to occur in layer-structured materials such as graphite and MXenes that can accommodate intercalation. Interestingly, it has also been recently claimed for the positive electrode of activated carbon that possessed a specific surface area (2070 $m^2\,g^{-1}$) which would have given a specific capacitance of up to 207 F g^{-1} assuming the EDL capacitance to be 10 μF/cm^2 on an ideal carbon surface. However, the reported specific capacitance was twice as large (419 F g^{-1}) in an inorganic ionic liquid, i.e. the molten eutectic mixture of $AlCl_3$-NaCl-LiCl at 125 °C. This increase in specific capacitance was attributed to reaction (12) because the XRD pattern of the activated carbon did exhibit a broad peak indicating the presence of graphitic structures.[200]

On the other hand, CVs of the full cell of the molten salts exhibited typical EDL capacitance at low cell voltages, and additional Faradaic storage at higher cell voltages.[200] Such features have been observed on the CVs of activated carbon supercapacitor cells containing aqueous iodide or bromide electrolytes as exemplified in Fig. 11c. Instead of intercalation, the enhanced storage at high voltages was attributed to the X^-/X_3^- couple according to reactions (9) and (10).[191,194]

An interesting phenomenon related to CVs similar to those in Figs. 11c and 11d is that such cells show two apparent capacitive storage mechanisms. It is reasonable to attribute the low voltage storage to EDL, but the high voltage storage should have involved the Nernstian mechanism according to either reactions (9) and (10) or reaction (12). However, it is not yet clear how these Nernstian reactions behave in a capacitive manner. It may be hypothesised that the porous activated carbon electrodes may offer widely distributed and energetically different Nernstian reaction sites, leading to the apparent capacitive behaviour. Alternatively, because both the X^- and X_3^- ions are adsorbed on the reaction sites of the carbon surface, they become part of the EDL structure, and hence are "conjugated" electronically and two-dimensionally inside the EDL, contributing to capacitive charging and discharging. The interfacial conjugation hypothesis seems to agree with the observation of current peaks at low cell voltages, as shown in Fig. 11d, when an electrolyte of higher iodide concentration was used in the same activated carbon supercapacitor.[194] In such a case, because the surface reaction sites are already fully occupied, the excess amounts of X^- and X_3^- ions undergo the electrode reaction in the conventional Nernstian manner.

Further studies are obviously needed to confirm the reasons behind the additional capacitive behaviour at high cell voltages due to the added halide ions. The additional storage capacity gained and the extended cell voltage are both practically meaningful. For example, combining the specific capacitance of over 400 F g^{-1} for activated carbon in the molten mixture of $AlCi_3$-NaCl-LiCl at 125 °C, and the high specific charge capacity of alkali metals, the specific energy of the supercapattery with a positive electrode of activated carbon and a negative electrode of sodium (Na) or lithium (Li) can reach 445 or 1111 Wh kg^{-1}, respectively.[201]

The above discussion has not considered the service durability of activated carbon supercapatteries with halide ions as the redox additives. One expected consequence of repeated cycles of de-/intercalation according to reaction (12) is the fatigue-induced degradation of the porous activated carbon. Also, the very positive

potential needed for oxidising Cl^- to Cl_3^- means a high oxidising power of Cl_3^-. This property was exploited for the oxidative dissolution of metals and alloys in ionic liquids[202] and can in principle affect the durability of activated carbon in supercapacitors. Further, the anodic formation of Cl_3^- is not favoured in aqueous electrolytes, nor in many organic solutions and ionic liquids, which means the need for better understanding to guide the selection of a desirable electrolyte. Last, but not the least, the specific capacitance and the correlated microstructure of activated carbon can vary significantly, depending on the manufacturing method, the electrolyte and its working temperatures.

In using an alkali metal negative electrode, it is desirable to select a working temperature at which the metal remains as a liquid to avoid the deposition of metal dendrites. The melting points are 180.5, 97.8 and 63.5 °C for Li, Na and K metals, respectively. Therefore, the prospect of using Na metal on the negative electrode and activated carbon on the positive electrode is very attractive in terms of performance, resources, cost, and working conditions. Alkaline earth metals have also relatively high charge capacities, but the melting points are much higher with 650.0 and 842.0 °C for Mg and Ca metals, respectively. There are many inorganic molten salts that are stable at the needed working temperatures in which carbon anodes are commonly used for electrolysis. The next step should be to study the structural stability of activated carbons so that their capacitive storage performance can be enhanced, maintained or at least is not compromised significantly.

5.2 Redox-active electrolytes

There is no doubt that the electrolytic solution is one of the crucial components of each electrochemical system. As a source of ions, this is even more profound in the case of electrochemical capacitors that are supposed to store charge by arranging ions in the so-called electric double-layer, formed at the electrode/electrolyte interface. Of course, the specific energy of traditional capacitors, based on double-layer storage, is not impressive, as it is a direct consequence of the double-layer capacitance, being estimated as up to 50 μF cm^{-2}.[203] Activated carbons as the electrodes with well-developed surface area (~1800 m^2 g^{-1}) and suitable micro/meso-porosity can ensure up to 20 Wh kg^{-1} at the device level.[203] On the one hand, this value is still far below the energy density for batteries. On the other hand, the specific power delivered by capacitors is remarkably higher than for the batteries (quite often up to 10 kW kg^{-1}), as there are no kinetic and diffusion-related limitations in the charging process. Furthermore, the cyclability of electrochemical capacitors is another factor that envisages them as a reasonable solution for fast and efficient energy storage.

As the electrode/electrolyte interface is a basic feature for all electrochemical processes, both components require thorough attention in the further development of device performance.[204] Interactions between the electrolytic solution and the electrode surface, especially surface functionalities, the interplay of electrode microtexture and electrolyte composition, electrolyte viscosity, reactivity, and thermal stability cannot be neglected in terms of many important aspects such as final capacitance value, operating voltage, self-discharge, leakage currents, or cyclability.[192] In addition, specific energy/power, rate handling, and charge propagation are derived from these parameters.

Redox-active electrolytes have been proposed as an alternative to pseudocapacitive electrode material such as RuO_x or MnO_x that allows high capacitance values and specific energy to be reached. Since the first work by Ishikawa et al. on brominated carbons and bromine[205–207] as well as Frackowiak et al. and others on iodides,[208–212] great progress has been made in the field. Research has expanded to other anionic redox-active electrolytes that contain halides (pseudohalides such as thiocyanate,[213] selenocyanate[214]), organometallic complexes (ferricyanide and ferrocyanide[215–222]) and organic anion – like indigo carmine[223] and many others.[192,224–226] Selected couples with their redox potentials have been presented in Fig. 12.[227]

There is widespread recognition that redox-active electrolytes have several advantages. The charge delivered by redox-active ions dissolved in the solution (or just a component of the redox-active ionic liquid without solvent) can be easily adjusted by the concentration of the specimen. This also impacts the conductivity of the solution and can have an impact on the redox potential. Furthermore, several redox-active species are soluble both in protic and aprotic media; therefore, they can boost the capacitance values for water-based systems and increase their specific energy, but also can serve as charge balancers in the organic environment and allow for a wider operating voltage window.

In addition to several advantages, redox-active electrolytes also have limitations. The redox-based charge storage mechanism on one electrode quite often induces faster self-discharge and triggers leakage currents, as the charged species are prone to the shuttling effect. In such a case, specially designed membranes or viscosity-modulated media that prevent the contact of species at different oxidation states are required.[224,226,228,229] In certain cases, mass balancing of the electrodes can be used to diminish the self-discharging process and retain the benefits from increased capacity.

Recently, it has been demonstrated that redox-active electrolytes could be successfully applied to hybrid metal-ion capacitors.[230] Their role in these systems is a bit different as the increased capacity

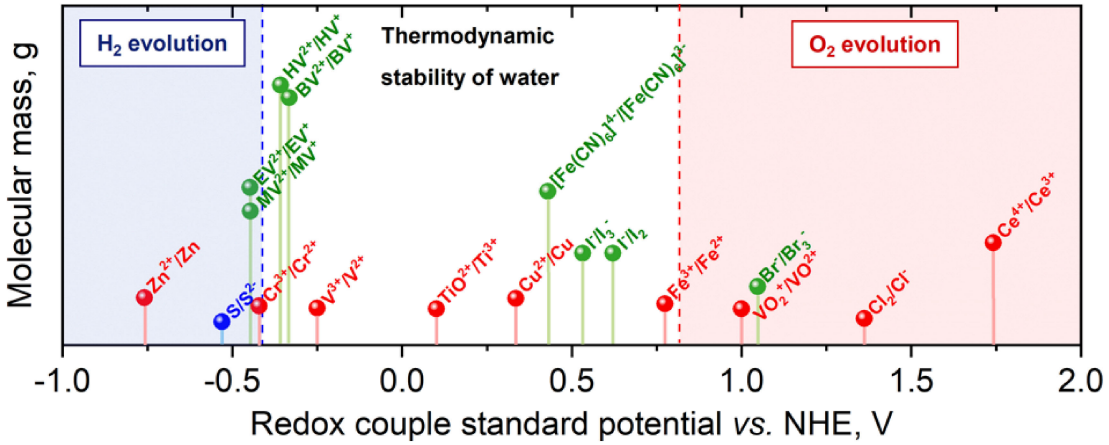

Figure 12. Redox couples with their formal potentials, based on Redox couples marked in red are stable under acidic conditions, those marked in green are stable in neutral solutions, and those marked in blue are stable in alkaline electrolytes,[227] reprinted with permission from Ref. 227. Copyright 2015 Aurhors, CC BY 4.0.

of one (positive) electrode allows for full insertion of a negative electrode by Li, Na, or K. In the past, it was required either to preinsert the negative electrode in one cell and then combine it with a (positive) capacitive electrode in another cell or to use a composite electrode of increased capacity (e.g. composed of sacrificial materials) to counterbalance the insertion charge. In the latter case, the sacrificial material produced a so-called 'dead mass' that affected the final specific energy. In the case of a redox-active electrolyte, the capacitor could be assembled in one step, without external pre-insertion or adding additional mass to the system.

The development of redox-active electrolytes is just emerging and a number of issues need to be addressed. For each system, the right concentration of redox active components must be verified and optimized, especially in terms of electrolyte viscosity, conductivity, and corrosion. The latter, in particular, could be very problematic, especially for highly concentrated formulations. In summary, redox-active electrolytes are an interesting alternative for pseudocapacitive materials, providing additional charge from the electrolytic solution. They allow higher capacitance values and specific energy to be reached, however, it is evident that further study and optimization are needed in order to benefit from full spectrum of their advantages.

CRediT Authorship Contribution Statement

Masanobu Chiku: Conceptualization (Lead), Writing – original draft (Lead), Writing – review & editing (Lead)
Mozaffar Abdollahifar: Conceptualization (Equal), Writing – original draft (Equal), Writing – review & editing (Equal)
Thierry Brousse: Conceptualization (Equal), Writing – original draft (Equal), Writing – review & editing (Equal)
George Z. Chen: Conceptualization (Equal), Writing – original draft (Equal), Writing – review & editing (Equal)
Olivier Crosnier: Conceptualization (Equal), Writing – original draft (Equal), Writing – review & editing (Equal)
Bruce Dunn: Conceptualization (Equal), Writing – original draft (Equal), Writing – review & editing (Equal)
Krzysztof Fic: Conceptualization (Equal), Writing – original draft (Equal), Writing – review & editing (Equal)
Chi-Chang Hu: Conceptualization (Equal), Writing – original draft (Equal), Writing – review & editing (Equal)
Paweł Jeżowski: Writing – original draft (Equal), Writing – review & editing (Equal)
Adam Maćkowiak: Writing – original draft (Equal), Writing – review & editing (Equal)
Katsuhiko Naoi: Writing – original draft (Equal), Writing – review & editing (Equal)
Nobuhiro Ogihara: Conceptualization (Equal), Writing – original draft (Equal), Writing – review & editing (Equal)
Naohisa Okita: Conceptualization (Equal), Writing – original draft (Equal), Writing – review & editing (Equal)
Masashi Okubo: Conceptualization (Equal), Writing – original draft (Equal), Writing – review & editing (Equal)
Wataru Sugimoto: Conceptualization (Equal), Writing – original draft (Equal), Writing – review & editing (Equal)
Nae-Lih Wu: Conceptualization (Equal), Writing – original draft (Equal), Writing – review & editing (Equal)

Conflict of Interest

The authors declare no conflict of interest in the manuscript.

References

1. S. Trasatti and G. Buzzanca, *J. Electroanal. Chem.*, **29**, A1 (1971).
2. J. Fortunato, M. B. Sassin, C. N. Chervin, J. F. Parker, R. H. DeBlock, C. A. Gorski, and J. W. Long, *J. Electrochem. Soc.*, **168**, 024505 (2021).
3. S. L. Kuo and N. L. Wu, *Electrochem. Solid-State Lett.*, **8**, A495 (2005).
4. W. Sugimoto, K. Yokoshima, K. Ohuchi, Y. Murakami, and Y. Takasu, *J. Electrochem. Soc.*, **153**, A255 (2006).
5. K. W. Nam, M. G. Kim, and K. B. Kim, *J. Phys. Chem. C*, **111**, 749 (2007).
6. J. K. Chang, M. T. Lee, and W. T. Tsai, *J. Power Sources*, **166**, 590 (2007).
7. M. Toupin, T. Brousse, and D. Bélanger, *Chem. Mater.*, **16**, 3184 (2004).
8. O. Ghodbane, F. Ataherian, N. L. Wu, and F. Favier, *J. Power Sources*, **206**, 454 (2012).
9. H. W. Chang, Y. R. Lu, J. L. Chen, C. L. Chen, J. F. Lee, J. M. Chen, Y. C. Tsai, P. H. Yeh, W. C. Chou, and C. L. Dong, *Phys. Chem. Chem. Phys.*, **18**, 18705 (2016).
10. S. Cheng, L. Yang, D. Chen, X. Ji, Z. J. Jiang, D. Ding, and M. Liu, *Nano Energy*, **9**, 161 (2014).
11. D. Chen, D. Ding, X. Li, G. H. Waller, X. Xiong, M. A. El-Sayed, and M. Liu, *Chem. Mater.*, **27**, 6608 (2015).
12. H. Y. Lee and J. B. Goodenough, *J. Solid State Chem.*, **144**, 220 (1999).
13. M. Toupin, T. Brousse, and D. Bélanger, *Chem. Mater.*, **14**, 3946 (2002).
14. N. Goubard-Bretesché, O. Crosnier, C. Douard, A. Iadecola, R. Retoux, C. Payen, M.-L. Doublet, K. Kisu, E. Iwama, K. Naoi, F. Favier, and T. Brousse, *Small*, **16**, 2002855 (2020).
15. K. Robert, D. Stiévenard, D. Deresmes, C. Douard, A. Iadecola, D. Troadec, P. Simon, N. Nuns, M. Marinova, M. Huvé, P. Roussel, T. Brousse, and C. Lethien, *Energy Environ. Sci.*, **13**, 949 (2020).
16. T. Brousse, D. Bélanger, and J. W. Long, *J. Electrochem. Soc.*, **162**, A5185 (2015).
17. P. Simon, Y. Gogotsi, and B. Dunn, *Science*, **343**, 1210 (2014).
18. C. N. Chervin, A. M. Lubers, J. W. Long, and D. R. Rolison, *J. Electroanal. Chem.*, **644**, 155 (2010).
19. V. Augustyn, P. Simon, and B. Dunn, *Energy Environ. Sci.*, **7**, 1597 (2014).
20. K. J. Griffith, A. C. Forse, J. M. Griffin, and C. P. Grey, *J. Am. Chem. Soc.*, **138**, 8888 (2016).
21. S. Deebansok, J. Deng, E. Le Calvez, Y. Zhu, O. Crosnier, T. Brousse, and O. Fontaine, *Nat. Commun.*, **15**, 1133 (2024).
22. Y. Zhu, S. Deedbansok, J. Deng, X. Wang, T. Brousse, F. Favier, and O. Fontaine, *Adv. Energy Mater.*, **14**, 2304317 (2024).
23. H. Wang, Z. Xu, Z. Li, K. Cui, J. Ding, A. Kohandehghan, X. Tan, B. Zahiri, B. C. Olsen, and C. M. B. Holt, *Nano Lett.*, **14**, 1987 (2014).
24. M. Abdollahifar, H.-W. Liu, C.-H. Lin, Y.-T. Weng, H.-S. Sheu, J.-F. Lee, M.-L. Lu, Y.-F. Liao, and N.-L. Wu, *Energy Environ. Mater.*, **3**, 405 (2020).
25. W. Li, J. Shao, Q. Liu, X. Liu, X. Zhou, and J. Hu, *Electrochim. Acta*, **157**, 108 (2015).
26. W. Yang, H. Eraky, C. Zhang, A. P. Hitchcock, and I. Zhitomirsky, *Chem. Eng. J.*, **483**, 149391 (2024).
27. M. S. Hong, S. H. Lee, and S. W. Kim, *Electrochem. Solid-State Lett.*, **5**, A227 (2002).
28. Y.-T. Weng, H.-A. Pan, R.-C. Lee, T.-Y. Huang, Y. Chu, J.-F. Lee, H.-S. Sheu, and N.-L. Wu, *Adv. Energy Mater.*, **5**, 1500772 (2015).
29. K.-T. Lee, J.-F. Lee, and N.-L. Wu, *Electrochim. Acta*, **54**, 6148 (2009).
30. K.-T. Lee, C.-B. Tsai, W.-H. Ho, and N.-L. Wu, *Electrochem. Commun.*, **12**, 886 (2010).
31. O. Ghodbane, J.-L. Pascal, and F. Favier, *ACS Appl. Mater. Interfaces*, **1**, 1130 (2009).
32. N. Nagarajan, H. Humadi, and I. Zhitomirsky, *Electrochim. Acta*, **51**, 3039 (2006).
33. T. Brousse, M. Toupin, R. Dugas, L. Athouël, O. Crosnier, and D. Belanger, *J. Electrochem. Soc.*, **153**, A2171 (2006).
34. S.-L. Kuo and N.-L. Wu, *J. Electrochem. Soc.*, **153**, A1317 (2006).
35. X. Zhang, X. Liu, Y. Zeng, Y. Tong, and X. Lu, *Small Methods*, **4**, 1900823 (2020).
36. W. Lu, L. Yan, W. Ye, J. Ning, Y. Zhong, and Y. Hu, *J. Mater. Chem. A*, **10**, 15267 (2022).
37. A. Zhang, R. Gao, L. Hu, X. Zang, R. Yang, S. Wang, S. Yao, Z. Yang, H. Hao, and Y.-M. Yan, *Chem. Eng. J.*, **417**, 129186 (2021).
38. T. Zhai, S. Xie, M. Yu, P. Fang, C. Liang, X. Lu, and Y. Tong, *Nano Energy*, **8**, 255 (2014).
39. Y. Fu, X. Gao, D. Zha, J. Zhu, X. Ouyang, and X. Wang, *J. Mater. Chem. A*, **6**, 1601 (2018).
40. S. Lee, G. Nam, J. Sun, J.-S. Lee, H.-W. Lee, W. Chen, J. Cho, and Y. Cui, *Angew. Chem.*, **128**, 8741 (2016).
41. P. Cui, Y. Zhang, Z. Cao, Y. Liu, Z. Sun, S. Cheng, Y. Wu, J. Fu, and E. Xie, *Chem. Eng. J.*, **412**, 128676 (2021).
42. J. P. Zheng and T. R. Jow, *J. Electrochem. Soc.*, **142**, L6 (1995).
43. J. P. Zheng, P. J. Cygan, and T. R. Jow, *J. Electrochem. Soc.*, **142**, 2699 (1995).
44. W. Sugimoto, K. Yokoshima, Y. Murakami, and Y. Takasu, *Electrochim. Acta*, **52**, 1742 (2006).
45. J. W. Long, D. Bélanger, T. Brousse, W. Sugimoto, M. B. Sassin, and O. Crosnier, *MRS Bull.*, **36**, 513 (2011).
46. T. Brousse, D. Bélanger, K. Chiba, M. Egashira, F. Favier, J. Long, J. R. Miller, M. Morita, K. Naoi, P. Simon, and W. Sugimoto, *Springer Handbook of Electrochemical Energy* (1st ed.) (Eds. C. Breitkopf and K. Swider-Lyons), Springer-Verlag Berlin Heidelberg, pp. 495–561 (2017).
47. L. D. Burke and O. J. Murphy, *J. Electroanal. Chem. Interfacial Electrochem.*, **96**, 19 (1979).
48. L. D. Burke and O. J. Murphy, *J. Electroanal. Chem. Interfacial Electrochem.*, **112**, 39 (1980).
49. P. Siviglia, A. Daghetti, and S. Trasatti, *Colloids Surf.*, **7**, 15 (1983).
50. W. Sugimoto, T. Kizaki, K. Yokoshima, Y. Murakami, and Y. Takasu, *Electrochim. Acta*, **49**, 313 (2004).
51. A. J. Salkind, *Techniques of Electrochemistry*, John Wiley, New York (1972).
52. D. A. McKeown, P. L. Hagans, L. P. L. Carette, A. E. Russell, K. E. Swider, and D. R. Rolison, *J. Phys. Chem. B*, **103**, 4825 (1999).

53. W. Dmowski, T. Egami, K. E. Swider-Lyons, C. T. Love, and D. R. Rolison, *J. Phys. Chem. B*, **106**, 12677 (2002).
54. K. Doblhofer, M. Metikos, Z. Ogumi, H. Gerischer, and M. Metikoš, *Ber. Bunsen-Ges. Phys. Chem.*, **82**, 1046 (1978).
55. W. Sugimoto, H. Iwata, K. Yokoshima, Y. Murakami, and Y. Takasu, *J. Phys. Chem. B*, **109**, 7330 (2005).
56. M. Forghani, A. P. Cameron, and S. W. Donne, *J. Electrochem. Soc.*, **168**, 050503 (2021).
57. C. Chabanier, E. Irissou, D. Guay, J. F. Pelletier, M. Sutton, and L. B. Lurio, *Electrochem. Solid-State Lett.*, **5**, E40 (2002).
58. W. Sugimoto, *Encyclopedia of Applied Electrochemistry*, Springer New York, New York, NY, p. 1813 (2014).
59. C. B. Arnold, R. C. Wartena, K. E. Swider-Lyons, and A. Pique, *J. Electrochem. Soc.*, **150**, A571 (2003).
60. S. Makino, Y. Yamauchi, and W. Sugimoto, *J. Power Sources*, **227**, 153 (2013).
61. Y. Murakami, S. Tsuchiya, K. Yahikozawa, and Y. Takasu, *J. Mater. Sci. Lett.*, **13**, 1773 (1994).
62. K. Chang, C. Hu, and C. Chou, *Chem. Mater.*, **19**, 2112 (2007).
63. M. Vuković and D. Čukman, *J. Electroanal. Chem.*, **474**, 167 (1999).
64. C.-C. Hu and Y.-H. Huang, *J. Electrochem. Soc.*, **146**, 2465 (1999).
65. C.-C. Hu, H.-R. Chiang, and C.-C. Wang, *J. Solid State Electrochem.*, **7**, 477 (2003).
66. C. Hu, M. Liu, and K. Chang, *J. Power Sources*, **163**, 1126 (2007).
67. Y. Takasu and Y. Murakami, *Electrochim. Acta*, **45**, 4135 (2000).
68. W. Sugimoto, T. Shibutani, Y. Murakami, and Y. Takasu, *Electrochem. Solid-State Lett.*, **5**, A170 (2002).
69. C.-C. Wang and C.-C. Hu, *J. Electrochem. Soc.*, **152**, A370 (2005).
70. M. Wohlfahrt-Mehrens, J. Schenk, P. M. Wilde, E. Abdelmula, P. Axmann, and J. Garche, *J. Power Sources*, **105**, 182 (2002).
71. B. Park, C. D. Lokhande, H. Park, K. Jung, and O. Joo, *Mater. Chem. Phys.*, **86**, 239 (2004).
72. J. P. Zheng and T. R. Jow, *J. Power Sources*, **62**, 155 (1996).
73. J. Zhang, D. Jiang, B. Chen, J. Zhu, L. Jiang, and H. Fang, *J. Electrochem. Soc.*, **148**, A1362 (2001).
74. M. Min, K. Machida, J. H. Jang, and K. Naoi, *J. Electrochem. Soc.*, **153**, A334 (2006).
75. K. Naoi, S. Ishimoto, N. Ogihara, Y. Nakagawa, and S. Hatta, *J. Electrochem. Soc.*, **156**, A52 (2009).
76. S. Makino, T. Ban, and W. Sugimoto, *Electrochemistry*, **81**, 795 (2013).
77. W. Sugimoto, H. Iwata, Y. Yasunaga, Y. Murakami, and Y. Takasu, *Angew. Chem., Int. Ed.*, **42**, 4092 (2003).
78. K. Fukuda, T. Saida, J. Sato, M. Yonezawa, Y. Takasu, and W. Sugimoto, *Inorg. Chem.*, **49**, 4391 (2010).
79. R. Saito, Y. Sato, D. Takimoto, S. Hideshima, and W. Sugimoto, *Electrochemistry*, **88**, 107 (2020).
80. S. Ardizzone, G. Fregonara, and S. Trasatti, *Electrochim. Acta*, **35**, 263 (1990).
81. J. Rishpon and S. Gottesfeld, *J. Electrochem. Soc.*, **131**, 1960 (1984).
82. A. Foelske, O. Barbieri, M. Hahn, and R. Kötz, *Electrochem. Solid-State Lett.*, **9**, A268 (2006).
83. R. S. Kate, S. A. Khalate, and R. J. Deokate, *J. Alloys Compd.*, **734**, 89 (2018).
84. S. H. S. Pai, S. K. Pandey, E. J. J. Samuel, J. U. Jang, A. K. Nayak, and H. Han, *J. Energy Storage*, **76**, 109731 (2024).
85. K. C. Liu and M. A. Anderson, *J. Electrochem. Soc.*, **143**, 124 (1996).
86. A.-L. Brisse, P. Stevens, G. Toussaint, O. Crosnier, and T. Brousse, *Materials*, **11**, 1178 (2018).
87. R. D. Noce, S. Eugénioa, M. Boudardbc, L. Rapennebc, T. M. Silvaad, M. J. Carmezimae, S. W. Donnef, and M. F. Montemor, *RSC Adv.*, **6**, 15920 (2016).
88. V. Srinivasan and J. W. Weidner, *J. Electrochem. Soc.*, **144**, L210 (1997).
89. W. G. Nunes, A. N. Miranda, B. Freitas, R. Vicentini, A. C. Oliveira, G. Doubek, R. G. Freitas, L. M. D. Silva, and H. Zanin, *Nanoscale*, **13**, 9590 (2021).
90. Z. Luo, L. Liu, X. Yang, X. Luo, P. Bi, Z. Fu, A. Pang, W. Li, and Y. Yi, *ACS Appl. Mater. Interfaces*, **12**, 39098 (2020).
91. J. Zhao, Y. Tian, A. Liu, L. Song, and Z. Zhao, *Mater. Sci. Semicond. Process.*, **96**, 78 (2019).
92. G. Bharathy and P. Raji, *Physica B*, **530**, 75 (2018).
93. Q. Wei, F. Xiong, S. Tan, L. Huang, E. H. Lan, B. Dunn, and L. Mai, *Adv. Mater.*, **29**, 1602300 (2017).
94. G. Cai, X. Wang, M. Cui, P. Darmawan, J. Wang, A. L. S. Eh, and P. S. Lee, *Nano Energy*, **12**, 258 (2015).
95. B. Zhao, J. Song, T. Fang, P. Liu, Z. Jiao, H. Zhang, and Y. Jiang, *Mater. Lett.*, **67**, 24 (2012).
96. H. Inoue, Y. Namba, and E. Higuchi, *J. Power Sources*, **195**, 6239 (2010).
97. M. Chiku, Y. Namba, E. Higuchi, and H. Inoue, *Electrochemistry*, **81**, 792 (2013).
98. M. Fan, B. Ren, L. Yu, Q. Liu, J. Wang, D. Song, J. Liu, X. Jing, and L. Liu, *CrystEngComm*, **16**, 10389 (2014).
99. U. M. Patil, R. R. Salunkhe, K. V. Gurav, and C. D. Lokhande, *Appl. Surf. Sci.*, **255**, 2603 (2008).
100. M. Chiku, M. Toda, E. Higuchi, and H. Inoue, *J. Power Sources*, **286**, 193 (2015).
101. M. Salanne, B. Rotenberg, K. Naoi, K. Kaneko, P. L. Taberna, C. P. Grey, B. Dunn, and P. Simon, *Nat. Energy*, **1**, 16070 (2016).
102. K. Naoi, W. Naoi, S. Aoyagi, J. Miyamoto, and T. Kamino, *Acc. Chem. Res.*, **46**, 1075 (2013).
103. K. Naoi, S. Ishimoto, J. Miyamoto, and W. Naoi, *Energy Environ. Sci.*, **5**, 9363 (2012).
104. K. Matsumura, E. Iwama, K. Takagi, N. Hashizume, Y. Chikaoka, N. Okita, W. Naoi, and K. Naoi, *J. Mater. Chem. A*, **11**, 1841 (2023).
105. K. Naoi, S. Ishimoto, Y. Isobe, and S. Aoyagi, *J. Power Sources*, **195**, 6250 (2010).
106. K. Kisu, M. Iijima, E. Iwama, M. Saito, Y. Orikasa, W. Naoi, and K. Naoi, *J. Mater. Chem. A*, **2**, 13058 (2014).
107. K. Naoi, T. Kurita, M. Abe, T. Furuhashi, Y. Abe, K. Okazaki, J. Miyamoto, E. Iwama, S. Aoyagi, W. Naoi, and P. Simon, *Adv. Mater.*, **28**, 6751 (2016).
108. E. Iwama, N. Kawabata, N. Nishio, K. Kisu, J. Miyamoto, W. Naoi, P. Rozier, P. Simon, and K. Naoi, *ACS Nano*, **10**, 5398 (2016).
109. P. Rozier, E. Iwama, N. Nishio, K. Baba, K. Matsumura, K. Kisu, J. Miyamoto, W. Naoi, Y. Orikasa, P. Simon, and K. Naoi, *Chem. Mater.*, **30**, 4926 (2018).
110. K. Matsumura, E. Iwama, Y. Tomochika, T. Matsuura, W. Naoi, and K. Naoi, *J. Electrochem. Soc.*, **170**, 010524 (2023).
111. T. Kondo, K. Matsumura, P. Rozier, P. Simon, K. Machida, S. Takeda, S. Ishimoto, K. Tamamitsu, E. Iwama, W. Naoi, and K. Naoi, *Chem. Mater.*, **36**, 2495 (2024).
112. K. Naoi, K. Kisu, E. Iwama, S. Nakashima, Y. Sakai, Y. Orikasa, P. Leone, N. Dupré, T. Brousse, P. Rozier, W. Naoi, and P. Simon, *Energy Environ. Sci.*, **9**, 2143 (2016).
113. K. Kisu, E. Iwama, W. Naoi, P. Simon, and K. Naoi, *Electrochem. Commun.*, **72**, 10 (2016).
114. Y. Orikasa, K. Kisu, E. Iwama, W. Naoi, Y. Yamaguchi, Y. Yamaguchi, N. Okita, K. Ohara, T. Munesada, M. Hattori, K. Yamamoto, P. Rozier, P. Simon, and K. Naoi, *Chem. Mater.*, **32**, 1011 (2020).
115. Y. Chikaoka, N. Nakata, K. Fujii, S. Sawayama, R. Ochi, E. Iwama, N. Okita, Y. Harada, Y. Orikasa, W. Naoi, and K. Naoi, *ACS Appl. Energy Mater.*, **6**, 4657 (2023).
116. K. Naoi, K. Kisu, E. Iwama, Y. Sato, M. Shinoda, N. Okita, and W. Naoi, *J. Electrochem. Soc.*, **162**, A827 (2015).
117. Y. Harada, N. Okita, M. Fukuyama, E. Iwama, W. Naoi, and K. Naoi, *J. Mater. Chem. A*, **12**, 1703 (2024).
118. Y. Harada, Y. Chikaoka, M. Kasai, K. Koizumi, E. Iwama, N. Okita, Y. Orikasa, W. Naoi, and K. Naoi, *J. Mater. Chem. A*, **12**, 2081 (2024).
119. N. Okita, E. Iwama, and K. Naoi, *Electrochemistry*, **88**, 83 (2020).
120. N. Okita, E. Iwama, S. Tatsumi, T. N. H. Võ, W. Naoi, M. T. H. Reid, and K. Naoi, *Electrochemistry*, **87**, 148 (2019).
121. Y. Chikaoka, R. Okuda, T. Hashimoto, M. Kuwao, W. Naoi, E. Iwama, and K. Naoi, *Electrochim. Acta*, **423**, 140558 (2022).
122. P. Novák, K. Müller, K. S. V. Santhanam, and O. Haas, *Chem. Rev.*, **97**, 207 (1997).
123. Y. Liang, Z. Tao, and J. Chen, *Adv. Energy Mater.*, **2**, 742 (2012).
124. H. Furukawa, K. E. Cordova, M. O'Keeffe, and O. M. Yaghi, *Science*, **341**, 1230444 (2013).
125. Z. Liang, C. Qu, W. Guo, R. Zou, and Q. Xu, *Adv. Mater.*, **30**, 1702891 (2018).
126. P. Poizot, J. Gaubicher, S. Renault, L. Dubois, Y. Liang, and Y. Yao, *Chem. Rev.*, **120**, 6490 (2020).
127. D. Banerjee, S. J. Kim, and J. B. Parise, *Cryst. Growth Des.*, **9**, 2500 (2009).
128. J. Heiska, M. Nisula, and M. Karppinen, *J. Mater. Chem. A*, **7**, 18735 (2019).
129. J. Kaduk, *Acta Crystallogr., Sect. B*, **56**, 474 (2000).
130. D. Banerjee and J. B. Parise, *Cryst. Growth Des.*, **11**, 4704 (2011).
131. N. Ogihara, T. Yasuda, Y. Kishida, T. Ohsuna, K. Miyamoto, and N. Ohba, *Angew. Chem., Int. Ed. Engl.*, **53**, 11467 (2014).
132. M. Armand, S. Grugeon, H. Vezin, S. Laruelle, P. Ribiere, P. Poizot, and J. M. Tarascon, *Nat. Mater.*, **8**, 120 (2009).
133. T. Yasuda and N. Ogihara, *Chem. Commun.*, **50**, 11565 (2014).
134. Y. Ozawa, N. Ogihara, M. Hasegawa, O. Hiruta, N. Ohba, and Y. Kishida, *Commun. Chem.*, **1**, 65 (2018).
135. R. Mikita, N. Ogihara, N. Takahashi, S. Kosaka, and N. Isomura, *Chem. Mater.*, **32**, 3396 (2020).
136. N. Ogihara, Y. Ozawa, and O. Hiruta, *J. Mater. Chem. A*, **4**, 3398 (2016).
137. N. Ogihara, N. Ohba, and Y. Kishida, *Sci. Adv.*, **3**, e1603103 (2017).
138. N. Ogihara, M. Hasegawa, H. Kumagai, and H. Nozaki, *ACS Nano*, **15**, 2719 (2021).
139. N. Ogihara, S. Kawauchi, C. Okuda, Y. Itou, Y. Takeuchi, and Y. Ukyo, *J. Electrochem. Soc.*, **159**, A1034 (2012).
140. N. Ogihara, Y. Itou, T. Sasaki, and Y. Takeuchi, *J. Phys. Chem. C*, **119**, 4612 (2015).
141. L. Fédèle, F. Sauvage, S. Gottis, C. Davoisne, E. Salager, J.-N. Chotard, and M. Becuwe, *Chem. Mater.*, **29**, 546 (2017).
142. H. Hazama, D. Murai, N. Nagasako, M. Hasegawa, and N. Ogihara, *Adv. Mater. Technol.*, **5**, 2000254 (2020).
143. N. Ogihara, M. Hasegawa, H. Kumagai, R. Mikita, and N. Nagasako, *Nat. Commun.*, **14**, 1472 (2023).
144. C.-C. Hu, W.-C. Chen, and K.-H. Chang, *J. Electrochem. Soc.*, **151**, A281 (2004).
145. C.-C. Hu and C.-C. Wang, *J. Electrochem. Soc.*, **150**, A1079 (2003).

146. K. Brezesinski, J. Wang, J. Haetge, C. Reitz, S. O. Steinmueller, S. H. Tolbert, B. M. Smarsly, B. Dunn, and T. Brezesinski, *J. Am. Chem. Soc.*, **132**, 6982 (2010).
147. H.-S. Kim, J. B. Cook, H. Lin, J. S. Ko, S. H. Tolbert, V. Ozolins, and B. Dunn, *Nat. Mater.*, **16**, 454 (2017).
148. S. Huang, L. Zhang, X. Lu, L. Liu, L. Liu, X. Sun, Y. Yin, S. Oswald, Z. Zou, and F. Ding, *ACS Nano*, **11**, 821 (2017).
149. W. M. Seong, K. Yoon, M. H. Lee, S.-K. Jung, and K. Kang, *Nano Lett.*, **19**, 29 (2019).
150. Y. Jiang and J. Liu, *Energy Environ. Mater.*, **2**, 30 (2019).
151. C.-W. Tai, Y.-T. Lu, T.-Y. Yi, Y.-C. Liu, Y.-S. Chen, and C.-C. Hu, *J. Electrochem. Soc.*, **170**, 040526 (2023).
152. S.-M. Li, S.-Y. Yang, Y.-S. Wang, H.-P. Tsai, H.-W. Tien, S.-T. Hsiao, W.-H. Liao, C.-L. Chang, C.-C. M. Ma, and C.-C. Hu, *J. Power Sources*, **278**, 218 (2015).
153. T.-Y. Yi, C.-W. Dai, J.-A. Wang, C.-C. M. Ma, and C.-C. Hu, *Electrochim. Acta*, **359**, 136941 (2020).
154. T. Ohta, I.-T. Kim, M. Egashira, N. Yoshimoto, and M. Morita, *J. Power Sources*, **198**, 408 (2012).
155. C.-W. Tai, W.-Y. Jao, L.-C. Tseng, P.-C. Wang, A.-P. Tu, and C.-C. Hu, *J. Mater. Chem. A*, **11**, 19669 (2023).
156. A. Adomkevicius, L. Cabo-Fernandez, T.-H. Wu, T.-M. Ou, M.-G. Chen, Y. Andreev, C.-C. Hu, and L. J. Hardwick, *J. Mater. Chem. A*, **5**, 10021 (2017).
157. M. Naguib, M. Kurtoglu, V. Presser, J. Lu, J. Niu, M. Heon, L. Hultman, Y. Gogotsi, and M. W. Barsoum, *Adv. Mater.*, **23**, 4248 (2011).
158. M. Naguib, O. Mashtalir, J. Carle, V. Presser, J. Lu, L. Hultman, Y. Gogotsi, and M. W. Barsoum, *ACS Nano*, **6**, 1322 (2012).
159. M. Ghidiu, M. R. Lukatskaya, M. Q. Zhao, Y. Gogotsi, and M. W. Barsoum, *Nature*, **516**, 78 (2014).
160. Y. Li, H. Shao, Z. Lin, J. Lu, L. Liu, B. Duployer, P. O. A. Persson, P. Eklund, L. Hultman, M. Li, K. Chen, X. H. Zha, S. Du, P. Rozier, Z. Chai, E. Raymundo-Pinero, P. L. Taberna, P. Simon, and Q. Huang, *Nat. Mater.*, **19**, 894 (2020).
161. V. Kamysbayev, A. Filatov, H. Hu, X. Rui, F. Lagunas, D. Wang, R. F. Klie, and D. V. Talapin, *Science*, **369**, 979 (2020).
162. D. Wang, C. Zhou, A. Filatov, W. Cho, F. Lagunas, M. Wang, S. Vaikuntanathan, C. Liu, R. F. Klie, and D. V. Talapin, *Science*, **379**, 1242 (2023).
163. S. Kajiyama, L. Szabova, H. Iinuma, A. Sugahara, K. Gotoh, K. Sodeyama, Y. Tateyama, M. Okubo, and A. Yamada, *Adv. Energy Mater.*, **7**, 1601873 (2017).
164. B. Anasori, M. R. Lukatskaya, and Y. Gogotsi, *Nat. Rev. Mater.*, **2**, 16098 (2017).
165. M. Okubo, A. Sugahara, S. Kajiyama, and A. Yamada, *Acc. Chem. Res.*, **51**, 591 (2018).
166. M. R. Lukatskaya, O. Mashtalir, C. E. Ren, Y. Dall'Agnese, P. Rozier, P. L. Taberna, M. Naguib, P. Simon, M. W. Barsoum, and Y. Gogotsi, *Science*, **341**, 1502 (2013).
167. O. Mashtalir, M. Naguib, V. N. Mochalin, Y. Dall'Agnese, M. Heon, M. W. Barsoum, and Y. Gogotsi, *Nat. Commun.*, **4**, 1716 (2013).
168. K. Kim, Y. Ando, A. Sugahara, S. Ko, Y. Yamada, M. Otani, M. Okubo, and A. Yamada, *Chem. Mater.*, **31**, 5190 (2019).
169. A. Sugahara, Y. Ando, S. Kajiyama, K. Yazawa, K. Gotoh, M. Otani, M. Okubo, and A. Yamada, *Nat. Commun.*, **10**, 850 (2019).
170. K. Kawai, Y. Ando, and M. Okubo, *Small Methods*, **2024**, 2400062 (2024).
171. Y. Ando, M. Okubo, A. Yamada, and M. Otani, *Adv. Funct. Mater.*, **30**, 2000820 (2020).
172. Y. Xia, T. S. Mathis, M. Q. Zhao, B. Anasori, A. Dang, Z. H. Zhou, H. Cho, Y. Gogotsi, and S. Yang, *Nature*, **557**, 409 (2018).
173. K. Kawai, M. Fujita, R. Iizuka, A. Yamada, and M. Okubo, *2D Mater.*, **10**, 014012 (2023).
174. L. Liu, H. Zschiesche, M. Antonietti, M. Gibilaro, P. Chamelot, L. Massot, P. Rozier, P.-L. Taberna, and P. Simon, *Adv. Energy Mater.*, **13**, 2203805 (2023).
175. T. Shimada, N. Takenaka, Y. Ando, M. Otani, M. Okubo, and A. Yamada, *Chem. Mater.*, **34**, 2069 (2022).
176. M. Naguib, J. Come, B. Dyatkin, V. Presser, P. L. Taberna, P. Simon, M. W. Barsoum, and Y. Gogotsi, *Electrochem. Commun.*, **16**, 61 (2012).
177. Y. Xie, Y. Dall'Agnese, M. Naguib, Y. Gogotsi, M. W. Barsoum, H. L. Zhaung, and P. R. C. Kent, *ACS Nano*, **8**, 9606 (2014).
178. X. Wang, S. Kajiyama, H. Iinuma, E. Hosono, S. Oro, I. Moriguchi, M. Okubo, and A. Yamada, *Nat. Commun.*, **6**, 6544 (2015).
179. S. Kajiyama, L. Szabova, K. Sodeyama, H. Iinuma, R. Morita, K. Gotoh, Y. Tateyama, M. Okubo, and A. Yamada, *ACS Nano*, **10**, 3334 (2016).
180. X. Wang, T. S. Mathis, K. Li, Z. Lin, L. Vlcek, T. Torita, N. C. Osti, C. Hatter, P. Urbankowski, A. Sarycheva, M. Tyagi, E. Mamontov, P. Simon, and Y. Gogotsi, *Nat. Energy*, **4**, 241 (2019).
181. P. P. Michałowski, M. Anayee, T. S. Mathis, S. Kozdra, A. Wójcik, K. Hantanasirisakul, I. Jóźwik, A. Piątkowska, M. Możdżonek, A. Malinowska, R. Diduszko, E. Wierzbicka, and Y. Gogotsi, *Nat. Nanotechnol.*, **17**, 1192 (2022).
182. J. Luo, X. Tao, J. Zhang, Y. Xia, H. Huang, L. Zhang, Y. Gan, C. Liang, and W. Zhang, *ACS Nano*, **10**, 2491 (2016).
183. R. Parsons, *Advances in Electrochemistry and Electrochemical Engineering* (Eds. P. Delahay and C. W. Tobias), Vol. 7, John Wiley & Sons, Inc., New York, p. 177 (1970).
184. A. J. Bard and L. R. Faulkner, *Electrochemical Methods: Fundamentals and Applications* (2nd ed.), John Wiley & Sons, Inc., New York (2001).
185. J. O. Bockris and H. Kita, *J. Electrochem. Soc.*, **108**, 676 (1961).
186. B. E. Conway, *J. Electrochem. Soc.*, **138**, 1539 (1991).
187. G. Z. Chen, *Prog. Nat. Sci.*, **31**, 792 (2021).
188. S. Fleischmann, J. B. Mitchell, R. Wang, C. Zhan, D. Jiang, V. Presser, and V. Augustyn, *Chem. Rev.*, **120**, 6738 (2020).
189. G. Z. Chen, *Int. Mater. Rev.*, **62**, 173 (2017).
190. T. Shimooka, S. Yamazaki, T. Sugimoto, T. Jyozuka, H. Teraishi, Y. Nagao, H. Oda, Y. Matsuda, and M. Ishikawa, *Electrochemistry*, **75**, 273 (2007).
191. G. Lota, K. Fic, and E. Frackowiak, *Electrochem. Commun.*, **13**, 38 (2011).
192. B. Akinwolemiwa, C. Peng, and G. Z. Chen, *J. Electrochem. Soc.*, **162**, A5054 (2015).
193. L. Guan, G. Z. Chen, A. K. Croft, and D. M. Grant, *J. Electrochem. Soc.*, **169**, 030529 (2022).
194. B. Akinwolemiwa, C. H. Wei, Q. H. Yang, L. P. Yu, L. Xia, D. Hu, C. Peng, and G. Z. Chen, *J. Electrochem. Soc.*, **165**, A4067 (2018).
195. E. Crawford, J. S. McIndoe, and D. G. Tuck, *Can. J. Chem.*, **84**, 1607 (2006).
196. H. J. Sun, L. P. Yu, X. B. Jin, X. H. Hu, D. H. Wang, and G. Z. Chen, *Electrochem. Commun.*, **7**, 685 (2005).
197. L. P. Yu, X. B. Jin, and G. Z. Chen, *J. Electroanal. Chem.*, **688**, 371 (2013).
198. H. B. Sun, W. Wang, Z. J. Yu, Y. Yuan, S. Wang, and S. Q. Jiao, *Chem. Commun.*, **51**, 11892 (2015).
199. M.-C. Lin, M. Gong, B. Lu, Y. Wu, D.-Y. Wang, M. Guan, M. Angell, C. Chen, J. Yang, B.-J. Hwang, and H. Dai, *Nature*, **520**, 324 (2015).
200. K. Wang, Z. Chen, K. Liu, C. Yang, H. Zhang, Y. Wu, Y. Long, H. Liu, Y. Jin, M. Li, and H. Wu, *Energy Environ. Sci.*, **15**, 5229 (2022).
201. Y. Yu, Y. H. Zhang, H. Wang, and G. Z. Chen, *Electrochemistry*, **92**, 043003 (2024).
202. X. H. Li, A. Van den Bossche, T. V. Hoogerstraete, and K. Binnemans, *Chem. Commun.*, **54**, 475 (2018).
203. F. Béguin and E. Frąckowiak, *Supercapacitors*, Wiley-VCH Verlag GmbH & Co. KGaA, Weinheim, Germany, p. 568 (2013).
204. B. Gorska, E. Frackowiak, and F. Beguin, *Curr. Opin. Electrochem.*, **9**, 95 (2018).
205. S. Yamazaki, T. Ito, Y. Murakumo, M. Naitou, T. Shimooka, M. Yamagata, and M. Ishikawa, *J. Power Sources*, **326**, 580 (2016).
206. K. Fic, S. Morimoto, E. Frąckowiak, and M. Ishikawa, *Batter. Supercaps*, **3**, 1080 (2020).
207. M. Maher, S. Hassan, K. Shoueir, B. Yousif, and M. E. A. Abo-Elsoud, *J. Mater. Res. Technol.*, **11**, 1232 (2021).
208. G. Lota and E. Frackowiak, *Electrochem. Commun.*, **11**, 87 (2009).
209. Y. Zhang, L. Zu, H. Lian, Z. Hu, Y. Jiang, Y. Liu, X. Wang, and X. Cui, *J. Alloys Compd.*, **694**, 136 (2017).
210. Z. Gao, L. Zhang, J. Chang, Z. Wang, D. Wu, F. Xu, Y. Guo, and K. Jiang, *Chem. Eng. J.*, **335**, 590 (2018).
211. S. T. Senthilkumar, R. K. Selvan, Y. S. Lee, and J. S. Melo, *J. Mater. Chem. A*, **1**, 1086 (2013).
212. K. V. Sankar and R. K. Selvan, *Carbon*, **90**, 260 (2015).
213. B. Gorska, P. Bujewska, and K. Fic, *Phys. Chem. Chem. Phys.*, **19**, 7923 (2017).
214. P. Bujewska, B. Gorska, and K. Fic, *Synth. Met.*, **253**, 62 (2019).
215. P. Iamprasertkun, A. Ejigu, and R. A. W. Dryfe, *Chem. Sci.*, **11**, 6978 (2020).
216. J. Lee, S. Choudhury, D. Weingarth, D. Kim, and V. Presser, *ACS Appl. Mater. Interfaces*, **8**, 23676 (2016).
217. G. K. Veerasubramani, K. Krishnamoorthy, and S. J. Kim, *J. Power Sources*, **306**, 378 (2016).
218. C. Lamiel, Y. R. Lee, M. H. Cho, D. Tuma, and J.-J. Shim, *J. Colloid Interface Sci.*, **507**, 300 (2017).
219. S. M. Cha, G. Nagaraju, S. C. Sekhar, and J. S. Yu, *J. Mater. Chem. A*, **5**, 2224 (2017).
220. N. R. Chodankar, D. P. Dubal, A. C. Lokhande, A. M. Patil, J. H. Kim, and C. D. Lokhande, *Sci. Rep.*, **6**, 39205 (2016).
221. A. Shanmugavani, S. Kaviselvi, K. V. Sankar, and R. K. Selvan, *Mater. Res. Bull.*, **62**, 161 (2015).
222. L.-H. Su, X.-G. Zhang, C.-H. Mi, G. A. O. Bo, and L. I. U. Yan, *Phys. Chem. Chem. Phys.*, **11**, 2195 (2009).
223. S. Roldán, Z. González, C. Blanco, M. Granda, R. Menéndez, and R. Santamaría, *Electrochim. Acta*, **56**, 3401 (2011).
224. L. B. Chen, H. Bai, Z. F. Huang, and L. Li, *Energy Environ. Sci.*, **7**, 1750 (2014).
225. J. Lee, P. Srimuk, S. Fleischmann, X. Su, T. A. Hatton, and V. Presser, *Prog. Mater. Sci.*, **101**, 46 (2019).
226. J. Lee, P. Srimuk, S. Fleischmann, A. Ridder, M. Zeiger, and V. Presser, *J. Mater. Chem. A*, **5**, 12520 (2017).
227. S.-E. Chun, B. Evanko, X. Wang, D. Vonlanthen, X. Ji, G. D. Stucky, and S. W. Boettcher, *Nat. Commun.*, **6**, 7818 (2015).
228. L. Q. Fan, J. Zhong, C. Y. Zhang, J. H. Wu, and Y. L. Wei, *Int. J. Hydrogen Energy*, **41**, 5725 (2016).
229. E. Frackowiak, K. Fic, M. Meller, and G. Lota, *ChemSusChem*, **5**, 1181 (2012).
230. A. Maćkowiak, P. Jeżowski, Y. Matsui, M. Ishikawa, and K. Fic, *Energy Storage Mater.*, **65**, 103163 (2024).